Current Research (2025) Newfoundland and Labrador Department of Industry, Energy and Technology Geological Survey, Report 25-1, pages 223-247

FINE-FRACTION INDICATOR MINERALOGY IN TILLS OVERLYING MINERALIZATION FROM NORTHEASTERN AND SOUTHWESTERN NEWFOUNDLAND: IMPLICATIONS FOR GOLD AND CRITICAL-MINERAL EXPLORATION

H.E. Campbell, J.S. Organ and J. Conliffe[1]
Terrain Sciences and Geoscience Data Management Section
[1]Mineral Deposits Section

ABSTRACT

*Twelve, 4–16-kg till samples, collected from stations overlying and down-ice of vein ultramafic and granite-hosted mineralization from northeast and southwest Newfoundland, were sent for heavy mineral analysis to IOS Geosciences in Chicoutimi, Québec. They were processed using a special fluidized bed and sieved to the <50 µm fraction to concentrate indicator minerals such as gold, precious metals and minerals (PMMs: platinum, osmium, ruthenium, stibiopalladinite and sperrylite), and granite-related mineral species (*i.e.*, Bi, Ta, Nb, Sn mineral species, scheelite and wolframite) for analysis. Till samples were also processed by shaking table, sieved to the 90–150 µm fraction and separated using 2.85 g/cm^3 and 3.2 g/cm^3 density liquids to concentrate indicator- and bedrock-mineral assemblages. The concentrates were then mounted and scanned using scanning electron microscopy (SEM) and automated classification methods identified the indicator minerals.*

Locally derived gold, chromite and PMMs, as well as distally derived granite minerals, were detected in the <50 µm fraction of till proximal to gold and chromite showings in northeast Newfoundland, and from the overlying pegmatites and down-ice of the potential mineral sources in southwest Newfoundland. Bedrock mineral assemblages from the 90–150 µm fraction were also indicative of the underlying bedrock, and of probable distal bedrock sources, located 10–30 km up-ice.

*The results demonstrated that mineral separation and automated detection methods were successful in identifying proximally derived mineralization and bedrock mineral assemblages in the fine fraction. Furthermore, abundant indicator minerals from distal up-ice sources indicate that SEM analysis and automated identification of indicator minerals in the fine fraction could be successfully employed in regional sampling studies (on the island) to detect mineralization in samples collected at sparse (*e.g.*, 10 km^2) grid densities.*

INTRODUCTION

Traditional geochemical analyses of till, at the Geological Survey of Newfoundland and Labrador's (GSNL) geochemical laboratory, have successfully identified local surface mineralization through anomalous gold- and base-metal mineralization, but elements associated with felsic and mafic intrusions (*i.e.*, Ta, W, Mo, Sn, Bi, Pt, Pd) often fall below the lab's detection capabilities, or are only detected in a small portion of samples (*see* GeoScience Atlas OnLine. March 2024. https://geoatlas.gov.nl.ca/). Furthermore, tracing bedrock sources from single-element till-geochemical anomalies is complicated by elemental similarities in source bedrock units.

To detect and trace detritus back to potential bedrock sources, optical identification of the coarse (>250 µm) fraction heavy-mineral assemblage has been used (*e.g.*, McClenaghan *et al.*, 2017; Plouffe *et al.*, 2024). These methods successfully identify indicator minerals, but the typical grain sizes of precious metals and minerals (PMMs) and Bi, Ta and Nb mineral species associated with ultramafic, and granite-hosted bedrock, are often too small to be detected optically (*e.g.*, Makvandi *et al.*, 2021). In addition, there are often only a few coarse-grained indicator minerals in samples, due to glacial comminution and mixing, hampering the interpretation of indicator mineral results from widely-spaced (*e.g.*, > 5 km^2) regional sample grids (*e.g.*, Campbell, 2024).

This study investigates the use of fine-fraction concentrations (<50 µm and 90–150 µm) coupled with automated detection methods to successfully identify indicator minerals in till samples. Study locations in northeast and southwest Newfoundland include: a) down-ice (?), but proximal

(1.5 km) to chromite mineralization at Burnt Pond (Figure 1A), b) down-ice proximal (0.15 km) of gold mineralization in Appleton (Figure 1A), c) directly overlying lithium–cesium–tantalum LCT-type pegmatites of the Kraken Prospect (Figure 1B) and, d) in an area of unknown mineral potential located 5 km east and northwest of gold showings near Ackerman Brook (Figure 1B).

SITE DESCRIPTIONS AND SAMPLE COLLECTION

Two areas (Figure 1A, B, Table 1) were investigated based on their proximity to mineral occurrences and their location within ice-flow paths, with two stations studied from each area. Some of the stations displayed complex soil profiles having multiple distinct till horizons. Where multiple till horizons were suspected, each till horizon was sampled and identified as Till A, Till B *etc.*; Till A representing the deepest sample (*e.g.*, Sample 2021JO5009A, *see* Table 1).

Two samples were collected at a station near Burnt Pond, overlying the Gander River Complex, ~1.5 km northwest of the chromite and asbestos showings (Blackwood, 1979). Six samples were collected from exposed till on the sides of exploration trenches located approximately 100–150 m northeast of gold-bearing veins hosted in shale north of Appleton (Sandeman and Honsberger, 2023; Eccles *et al.*, 2024). Three samples were collected from two tills overlying the East Dyke and Hockey Stick Dyke, along with a spodumene-rich bedrock sample at the Kraken Prospect in southern Newfoundland (Conliffe *et al.*, 2024), and one sample at a station near Ackerman Brook, 1.5 km northwest of the Couteau Brook showing (Figure 1, Table 1) in southwestern Newfoundland (Chorlton, 1980a, b; O'Brien and O'Brien, 1989).

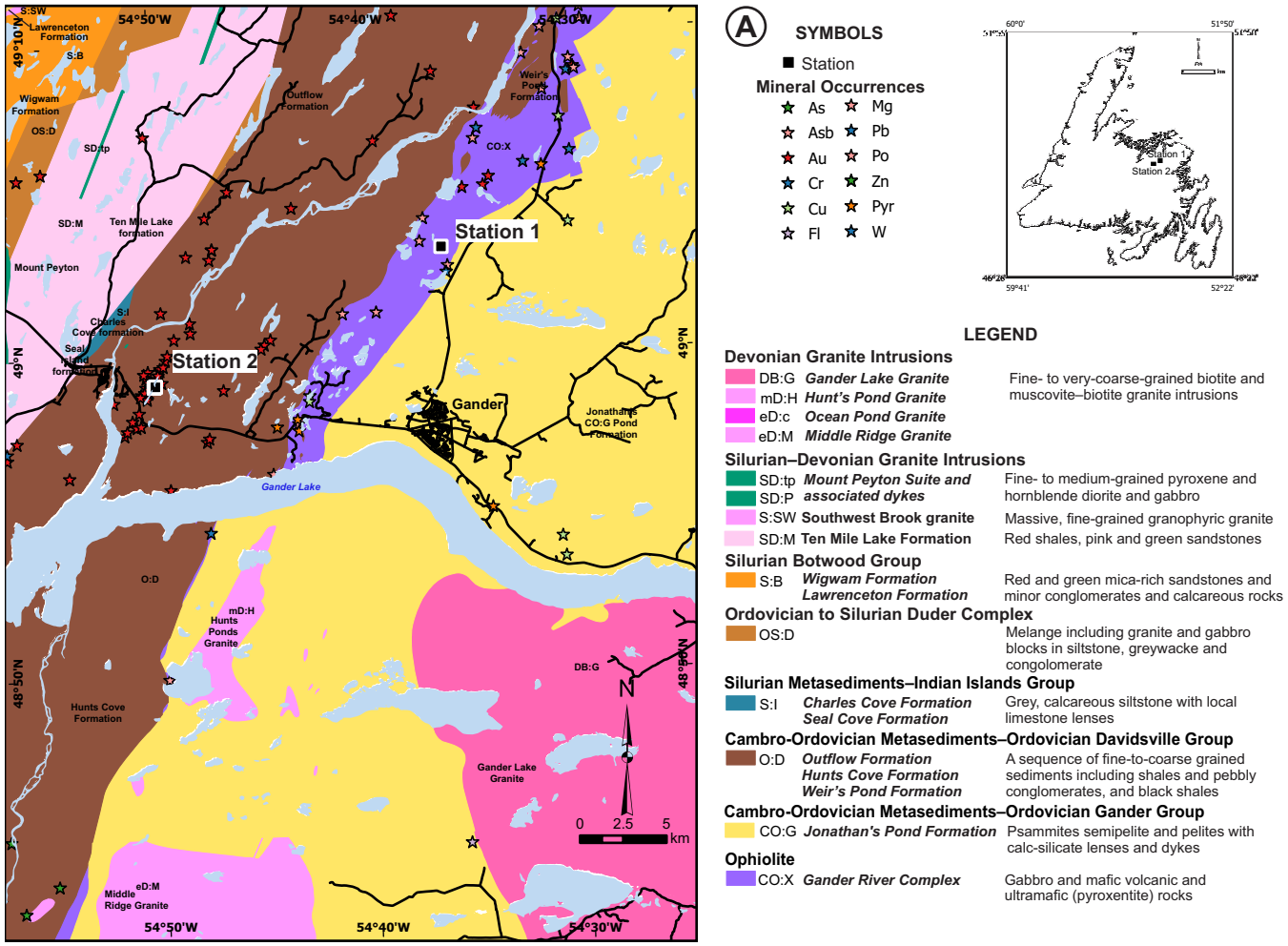

Figure 1. *A) Location map and simplified geological map for stations 1 and 2 (Burnt Pond and Appleton) and B) Stations 3 and 4 (Kraken Prospect and Ackerman Brook). The geological maps are derived from Colman-Sadd,* et al.*, 1990.*

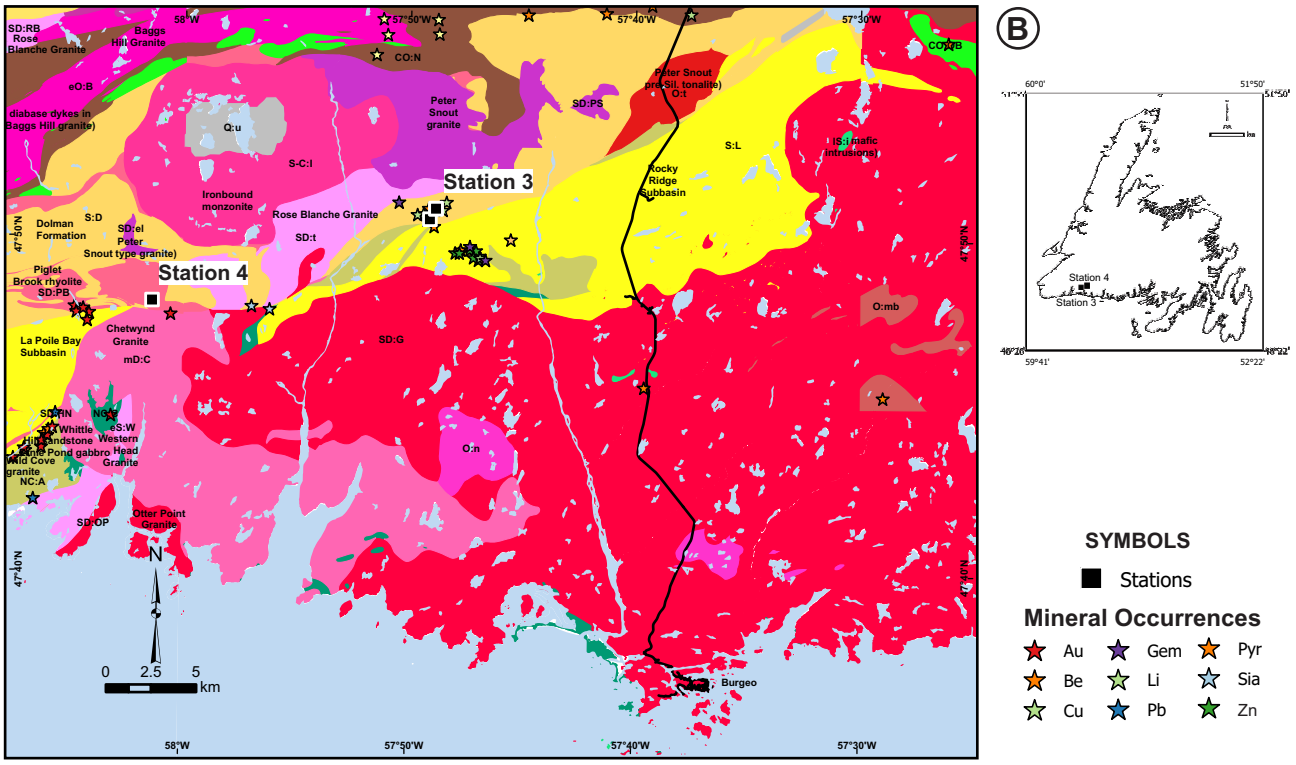

LEGEND

Q:u		Unconsolidated sediments
Late Silurian to Mississippian		
S-C:I	***Ironbound Hill Monzonite***	Medium-to-coarse-grained porphyritic granite and monzonite
Silurian–Devonian		
mD:C	***Chetwynd Granite***	Middle Devonian pink, fine- to medium-grained equigranular biotite granite with minor porphyritic phases
SD:PS	***Peter Snout Granite***	Massive fine-to-medium-grained, equigranular, biotite and muscovite granite, locally garnetiferous
SD:t SD:RB	***Rose Blanche Granite***	Foliated granodiorite, tonalite and muscovite-bearing granite with or without garnet and biotite; includes units thought to be equivalent to the Rose Blanche Granite
SD:PB	***Piglet Brook Rhyolite***	Pink, fine-grained rhyolite
SD:el		Medium- to fine-grained equigranular leucogranite with minor muscovite and garnet
eS:W	***Western Head Granite***	Buff, black and white, medium grained, equigranular biotite hornblende granodiorite with diorite xenoliths
SD:OP	***Otter Point Granite***	Pale pink and buff coarse-grained K-feldspar porphyritic bioite megacrystic granite
SD:G	***Burgeo Intrusive Suite***	K-feldspar and plagioclase porphyritic granodiorite and granite, biotite, muscovite granite
IS:i		Silurian mafic intrusions
Silurian		
S:D	***Dolman Cove Formation***	Felsic tuff and minor sandstone, shale, conglomerate and amphibolite
La Poile Group		
S:L	***Phillips Brook Rhyolite*** ***Gallyboy Harbour Tuff*** ***Cross Gulch Tuff***	Breccia composed of flow-banded rhyolite fragments Medium- to coarse-grained locally layered and stratified quartz-feldspar crystal tuff Multicoloured lithic tuff with felsic volcanic fragments
O:mb		Ordovician paragneiss, amphibolie and granitoid rocks-recrystallized
O:n		Ordovician grey, fine grained nebulitic hornblende granite
Cambrian to Ordovician		
eO:B	***Baggs Hill Granite***	Granophyre, quartz and quartz feldspar porphyry, granite and granodiorite
CO:N	***Bay du Nord Group***	Slate, quartzite, greywacke, conglomerate and minor limestone
CO:OB		Unnamed ophiolite in the Bay du Nord Group. Sheared and deformed lenticular mafic and ultramafic units including gabbro, dunite, pyroxenite and diabase
La Poile Basement Rocks (low grade)		
NC:A	***Roti Intrusive Suite***	Coarse-grained equigranular, blue quartz-bearing granodiorite
NC:C	***Cinq Cerf Gneiss***	Banded amphibolitic gneiss, hornblendite, and schist

Figure 1. *Continued.*

Table 1. Station and sample locations from northeastern and southwestern Newfoundland. Trench numbers and names are provided where multiple sections were sampled from one station

Station	Area	Sample	Trench number or name	Depth to bedrock	Easting (NAD27 Zone 21)	Northing (NAD27 Zone 21)	Elevation (m)	Bottom sample depth (m)	Till
1	Burnt Pond	2021JO5009A		0.80	675080	5436254	106	0.60	A
1	Burnt Pond	2021JO5009B		0.80	675080	5436254	106	0.20	B
2	Appleton	2021JO5019A	1	3.00	658496	5428059	105	3.00	A
2	Appleton	2021JO5019B	1	3.00	658496	5428059	105	2.00	B
2	Appleton	2021JO5019C	1	3.00	658496	5428059	105	1.3	C
2	Appleton	2021JO5020A	2	3.00	658565	5428107	113	2.55	A
2	Appleton	2021JO5020B	2	3.00	658565	5428107	113	1.60	B
2	Appleton	2021JO5020C	2	3.00	658565	5428107	113	0.80	C
3	Kraken Prospect	23JO5004	East Dyke	0.70	438832	5299223	229	0.50	B
3	Kraken Prospect	23JO5005	Hockey Stick Dyke	1.60	439112	5299603	271	1.40	A
3	Kraken Prospect	23JO5006	Hockey Stick Dyke	1.60	439112	5299603	271	0.65	B
4	Ackerman Brook	23JO5002		0.80?	423455	5294778	268	0.80	A

STATION 1: BURNT POND

Station 1 (Table 1, Sample 2021JO5009A) is located north of Burnt Pond, 2 km west of Jonathan's Pond provincial park (Figure 1A). The topography comprises north-northeastward trending ridges, valleys and bogs, and small brooks and rivers that drain northward into Gander River; the highest nearby hill is at 137 masl. Two, thin till horizons were identified based on field observations (Plate 1A) with relatively well-exposed bedrock in roadside ditches. A nearby multidirectional striation site records eastward (080°), northeastward (040°) and northward (003°) ice flows (Plate 1B). The Burnt Pond Point chromite indication (MODS 002E/02/Cr003) and the West Pond asbestos showing (MODS 002E/02/Asb005) are hosted in serpentinized ultramafic rocks and located up-ice of northwest and southeast ice flow directions identified in the region. The nearby bedrock units include medium- to coarse-grained pyroxenite, and minor serpentinite, magnesite, amphibolite, hornblendite and gabbro of the Gander River Complex (Blackwood, 1980; Figure 1A) of the Gander River Complex.

Sample 2021JO5009A (Table 1, Plate 1A) was collected at 0.60 mm, composed of a brown-grey fissile, compact till, with isolated silty sand stringers throughout and a dark-brown silty sand covering on (mafic?) clasts. Sample 2021JO5009B (Plate 1A) was collected at 0.20 m, above an undulating contact with the basal till, and is composed of grey silty to fine-grained sand diamicton having a slightly lower clast content. Clasts in the vicinity of the station range from sand to boulder size, with several large (>2 m) ultramafic boulders noted.

STATION 2: APPLETON

Station 2 is located 1.7 km north of the Trans-Canada Highway (TCH) and the town of Appleton (Figure 1A). The site is accessed from Simms Road, on the southeast corner of a pond along the "Appleton Linear", a >10 km northeast trending feature hosting numerous gold occurrences that are currently being explored by Newfound Gold Corporation at their Queensway property (Eccles *et al.*, 2024), as well as other junior exploration companies. The topography is defined by low-lying north–south trending ridges, valleys and bogs, with northward drainage into Gander River; a 139 masl ridge defines the highest local elevation.

Six samples were collected from the exposed walls of two (industry-dug) trenches at this station. The southernmost trench that includes samples 2021JO5019A-C (Table 1) is located 150 m northeast of the transmission line corridor. The second trench, that includes samples 2021JO5020A-C (Table 1) is located 100 m northeast, and upslope, of the first trench.

The ice-flow chronology, determined by striation measurements, indicates an older southeast flow, identified 2 km from the station, followed by younger northeast, and then northward flows (St. Croix and Taylor, 1991; Organ, 2022). Till in the immediate vicinity of the station is moderately thick (>2 m) and is locally observed to be composed of up to three distinct till units within a single soil profile, consisting of a lodgement till (Till A) overlain by deformation/lodgement tills (Tills B and C). In trench 1 (Table 1), the upper tills have been remobilized (Organ, 2022). Glacially and periglacially deformed bedrock and shale-rich diamicton and till are common throughout the region (Campbell *et al.*, 2022).

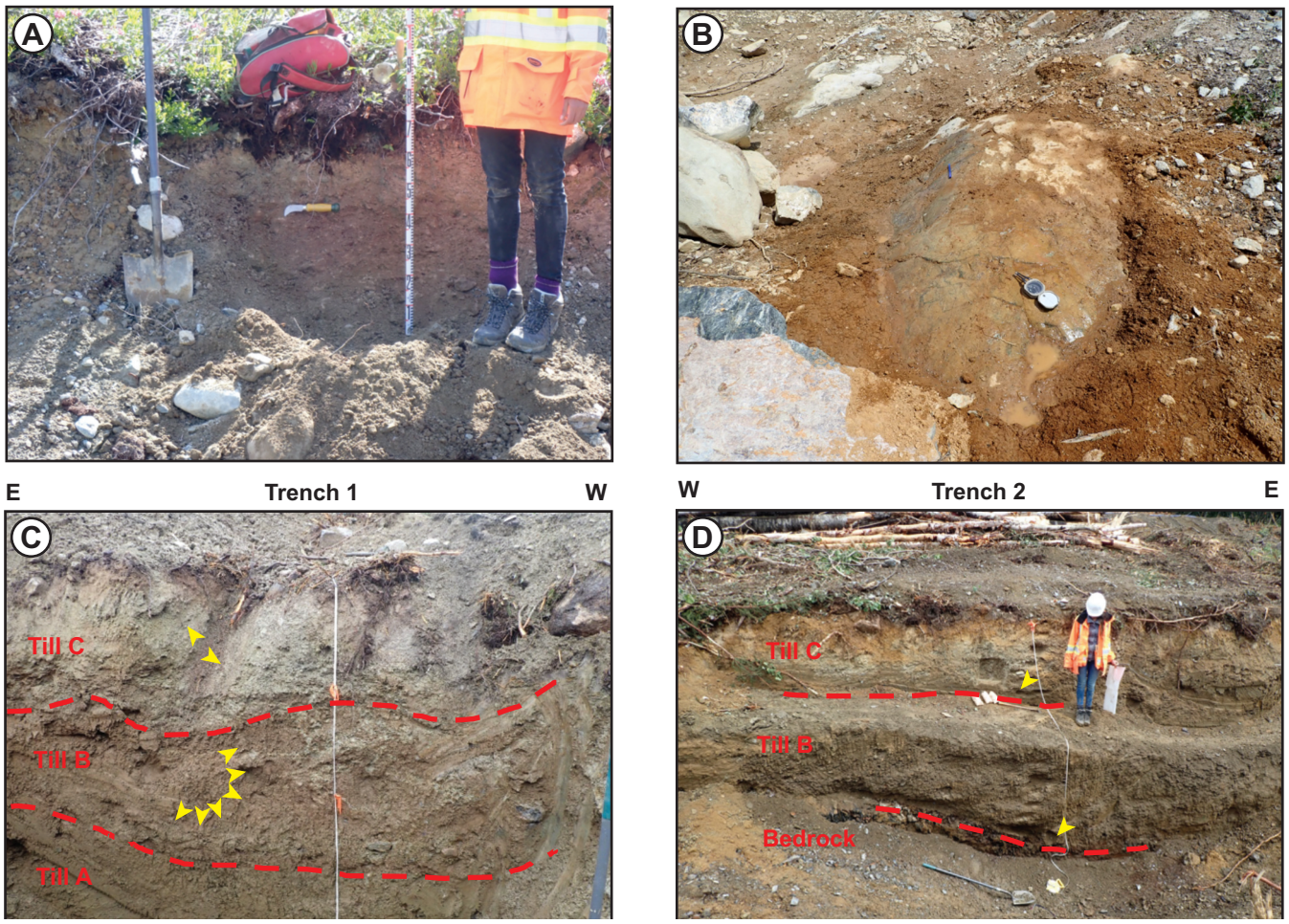

Plate 1. *A) Two till layers (separated by utility knife) in the Burnt Pond region of central Newfoundland; B) Striation site near Burnt Pond; C, D) Multiple tills (red dashed lines) from trenches north of Appleton. The small arrowheads represent the dip direction of the clasts in the different tills, looking southward in C and northward in D (*see *Organ* et al.*, 2022).*

Mineralization in the area includes gold-bearing quartz–carbonate veins hosted in isoclinally folded, steeply northwest-dipping, turbiditic sandstone sequences of the Outflow Formation and siltstones and shales of the Hunts Cove Formations that together comprise the Ordovician Davidsville Group (O'Neill and Blackwood, 1989). High-grade gold occurrences and visible gold grains are reported in this area (Eccles *et al.*, 2024). The Iceberg Zone (MODS 002D/15/Au038) and Golden Joint (MODS 002D/15/Au027) prospects occur northwest of the station location, and the Keats North Prospect (MODS 002D/15/Au033) occurs to the southwest.

Sample 2021JO5019A (Plate 1C) was collected from the base of trench 1 at 3 m, and is composed of a compact pale brown, indurated fine-grained silty-sand till, with angular to rounded, variably striated 0.2–20 cm long clasts, derived primarily from the underlying Davidsville Group, and the Mount Peyton Intrusive Suite (*e.g.*, Dickson, 1993), located 15 km to the southwest. This till (Till A) grades upwards, and at 2 m it changes to a poorly sorted, brown-grey to reddish-brown, silty-sand compact till (Sample 2021JO5019B), with observed clast contents similar to Till A. Sample 2021JO5019C from (1.3 m) is composed of a loosely consolidated, but moderately fissile, pale-brown silty sand with low clast content and a fine-grained matrix. It includes pebbles and cobbles of muscovite–biotite granite that resemble the Hunts Pond Intrusion, located 15 km south-southwest of the station (O'Neill and Colman-Sadd, 1993; Organ, 2022).

Sample 2021JO5020A was collected 2.55 m below the surface in trench 2. Vertically oriented angular to subrounded shale clasts, up to 10 cm in length, are incorporated from the bedrock into variably compact and fissile till that is similar in composition to Till A from trench 1. Sample 2021JO5020B was collected at 1.6 m depth from a compact and fissile silty sand matrix with 0.2–10 cm very angular to

subrounded clasts derived from the underlying Davidsville Group, and the Mount Peyton Intrusive Suite to the southwest; similar to Till B in trench 1. The upper most sample (2021JO5020C) was collected at 0.80 m depth, from a brown till above a sharp contact with Till B. Oxidation occurs throughout this till horizon, possibly due to plant rootlets. Clasts predominantly range from 0.2–2 cm, with some larger (10 cm) flat, subangular to subrounded clasts.

Fabrics measured at trench 2 show northward (Till B) and northeastward (Till C) clast orientations. These fabrics align with the known northward ice-flow directions determined from striations measured in this region; but they occur in reverse stratigraphic order than in the chronology presented by striations (*e.g.*, St. Croix and Taylor, 1991). The strong fabrics, along with the abundance of locally derived clasts, suggests they are lodgement tills that have been subglacially ploughed and deformed into a hard substrate (*e.g.*, Evans *et al.*, 2006).

STATION 3: KRAKEN PROSPECT

Three samples from Station 3 were collected from the exposed walls of the East Dyke and Hockey Stick trenches located 500 m from each other at the recently discovered Kraken Prospect (Conliffe *et al.*, 2024) located 30 km north-northwest of Burgeo and 11 km west of the Burgeo Highway (Figure 1B, Table 1). The station is accessed by helicopter and lies at the southern end of a relatively flat, barren 350 masl. plateau with streams and brooks flowing southward into Barasway and Connoire bays. Fluted landforms that are up to 2-km long, 400-m wide and 30-m high converge toward the bays from the proposed ice divide (*e.g.*, Shaw *et al.*, 2006) south of Spruce Pond in the east, and at the northern headwaters of La Poile River to the west (Sparkes, 1989; Sparkes and McCuaig, 2005). The trenches were excavated in shallow, bouldery northeast-to-southwest-oriented curvilinear till ridges that are interspersed with bogs (Plate 2A). Boulders and cobbles are common on the surface near, and in, till from the excavated trenches. Two striation measurements were collected from bedrock at the Hockey Stick Dyke trench, recording a 135° striation preserved in the lee of a younger, southerly directed (195°) striation.

The steeply dipping, northeast-trending pegmatite dykes at the Kraken Prospect are hosted in amphibolite-facies metamorphic rocks of the Dolman Cove Formation, with the peraluminous Rose Blanche Granite outcropping less than a kilometre away. The pegmatites contain spodumene, quartz, albite, muscovite, spessartine garnets (a manganese-rich garnet that commonly occurs within pegmatites) and columbite–tantalite with niobium-rich cores and Ta-rich rims (Conliffe *et al.*, 2024). Tourmaline is abundant in the host rocks proximal to the pegmatite dykes. A bedrock sample was collected from the spodumene-bearing East Dyke for mineralogical comparisons to the collected till samples.

Sample 23JO5004 was collected at 50 cm depth from the East Dyke trench (Figure 1B, Table 1). The till is sandy and contains abundant angular to subrounded large (1–2 m) boulders and cobbles (including spodumene-rich pegmatite boulders) and >20 %, 0.3–2 cm angular to subangular clasts of pegmatite, granite, amphibolite, and tuff (Plate 2B). Till toward the base of the trenches is sandier and more oxidized than the till in the upper part, and was therefore avoided during sampling.

Two samples were collected from till overlying the Hockey Stick Dyke. Sample 23JO5005 was collected at 1.4 m depth from the surface from a medium-compacted till with low clast content, immediately overlying interbedded mafic and felsic tuffs of the Dolman Cove Formation that are intruded by the spodumene-bearing pegmatite dyke (Plate 2C; Conliffe *et al.*, 2024). Sample 23JO5006 was collected at 0.65 m from a compact fissile silty sand till (Sample 23JO5006, Plate 2D). Angular, striated boulders and cobbles are noted in and around the trench, and a 10–20 cm angular schist and boulder raft appears on the eastern margin of the trench.

STATION 4: ACKERMAN BROOK

Station 4 (Table 1, Figure 1B) is located directly east of the headwaters of Ackerman Brook, 15 km east-southeast from the Kraken Prospect. It is on a plateau, 3.6 km south of the headwaters of Couteau Brook and 7.2 km north of the head of Couteau Bay. The site occurs directly south of a 1.7-km-long, north–south trending, linear glacial landform (*see* previous section; Sparkes, 1989; Sparkes and McCuaig, 2005; Plate 3A). Abundant frost-heaved blocks of rhyolite (Plate 3B) are noted. Till cover surrounding the linear landforms is thin to non-existent (Sparkes, 1989; Sparkes and McCuaig, 2005; Plate 3A). A south-trending striation (Plate 3C) measurement was collected 3 km north of the station.

The underlying bedrock is composed of fine-grained pink Piglet Brook rhyolite (Chorlton, 1980 a, b; O'Brien and O'Brien, 1989). Up-ice (north), the geology includes metasedimentary and metavolcanic rocks of the Dolman Cove Formation and Bay d'Est Group, as well as several peraluminous granite intrusions, and the Ironbound Hill monzonite (O'Brien and O'Brien, 1989). A number of gold occurrences are located close to the station, including the Couteau Brook Au showing (MODS 0010/16/Au007) approximately 1.5 km to the southeast and the Cross Gulch showings (Cross Gulch #1-3; MODS 011O/16/Au 001-003) 4 km to the west-southwest. Other nearby (<10 km) mineral

Plate 2. *A) Bog and ridge terrain typical of southwestern Newfoundland; B) Till section above the East Dyke trench; C) Amphibolite and pegmatite at the Hockey Stick Dyke; D) Till section above the Hockey Stick Dyke.*

occurrences include uranium showings to the east, hosted in the Dolman Cove Formation (Troy's Pond and ST-129 showings).

Sample 23JO5002 (Till A) was collected 0.8 m below the surface beneath an organic mat (Plate 3B), from a fine-grained grey-brown silty sand diamicton that liquefied during collection. The sample was very cold to the touch and may have been frozen during the winter months, possibly part of a discontinuous permafrost layer in till at higher elevations in southern Newfoundland (Liverman *et al.*, 2000). Very little textural data were observed at the site due to the liquefaction of sediment. Historical descriptions indicate that similar linear landforms are comprised of silt and clay cores that are mantled by a <1 m cover of sandy melt-out till (Sparkes, 1989).

ANALYTICAL METHODS

The samples were shipped to IOS Geosciences processing facilities in Chicoutimi, Québec (https://iosgeo.com/fr/accueil) for processing and detection of minerals using scan-

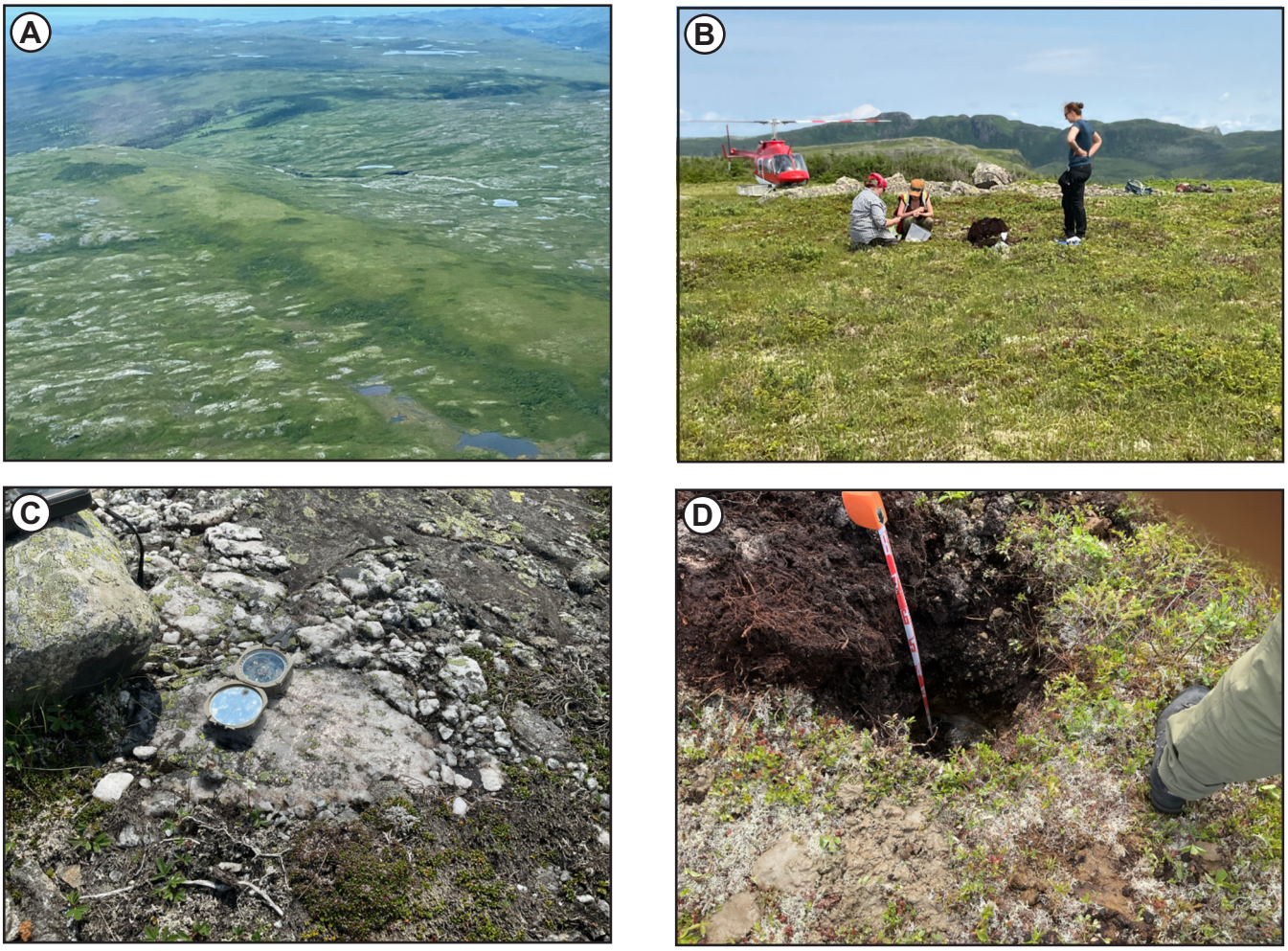

Plate 3. *A) A fluted (1 km long, 0.1 km wide) north-south trending ridge, similar to the ridge where the sample was collected; B) Sample site with frost-heaved bedrock in the background near the helicopter; C) Till sample site showing pale grey silty sand diamicton on the ground around the pit; D) A southward striation on an outcrop 3 km north of the station.*

ning electron microscopy-mineral liberation analysis (SEM-MLA). As this study was designed to test whether the relevant minerals could be identified in till collected proximal to known mineral occurrences, no detailed geological information was provided except for a discussion about the viability of retaining and identifying indicator minerals associated with LCT-type pegmatite and granite mineralization in the fine till fraction (*e.g.*, columbite–tantalum, niobium). The following discussions of the ARTGold and ARTMin analytical methods used by IOS to detect minerals in the <50 µm and 90–150 µm of till respectively, are based on personal communication with Rejean Girard, Natacha Fournier and Jonathan Trembley of IOS Geosciences.

Scanning electron microscopy-mineral liberation analysis (SEM-MLA: Gu, 2003) can rapidly and accurately detect minerals and their abundances in a single sample, by using a combination of back-scattered electron imagery and spectral signatures from scans of grains, including gold, silver, precious minerals and metals (PMMs), and other minerals in the fine fraction of till (Girard *et al.*, 2021a, b, Lougheed *et al.*, 2021; Makvandi *et al.*, 2021; Layton-Matthews and McClenaghan, 2022). Backscattered electrons from the sample scans are collected on a screen, producing an image. The interaction between electrons and the samples generate characteristic X-rays that can be integrated with the images to identify specific mineral phases (Sylvester, 2012). This method overcomes the limitations of optical grain identification; namely relying on the optically identifiable coarser fraction (>250 µm), identification bias, and expertise of the individual operator (Girard *et al.*, 2021a).

SAMPLE PREPARATION

Both the ARTGold and ARTMin analytical methods employ density separation using a shaking table; ARTGold

includes an additional preconcentration of the sample using a specially designed fluidized bed that is mounted as a feeder to the shaking table. The separates are sieved to the <50 µm fraction, to be scanned for gold, PMMs and other minerals (*e.g.*, Ta, Bi and Nb mineral species, scheelite and wolframite) associated with LCT-type pegmatites. ARTMin employs the shaking table separation, sieving to the 90–150 µm fraction and heavy and medium density liquid separation (>3.2 g/cm^3 and 2.85 g/cm^3), to detect minerals associated with the surrounding bedrock. Figure 2 shows a general workflow for sample preparation process. In addition to mineral identification, grain size analysis was also performed on a 300 g aliquot of the <1 mm sample.

ANALYTICAL QUALITY CONTROL

IOS Geosciences monitors the analytical procedures by examining material losses and the measurement of certified reference materials for the particle size analyzer. For the ARTGold results returning counts of more than 4 grains in the >50 µm fraction, a recount was performed. For the <50 µm fraction, the rejected tailings of one sample (2021JO5019C), were scanned for gold grains to determine the recovery rate of the fluidized bed during the first round of analysis. Similarly, for ARTMin, the rejected tailings from one sample (2021JO5020A), were rescanned and compared to the first sample scan for quality control. Consistent recovery rates are difficult to achieve for some minerals, largely related to variable mineral shapes (*e.g.*, tabular and prismatic minerals are less consistent in recovery, while rounded, stocky minerals are consistently recovered).

Grain size recoveries are between the upper and lower limits for the standard F500 powder used for grain size analysis. Tolerance for losses were determined by the sum of the weighting scale precision (Natacha Fournier, pers. comm., 2025). Half the sample weight was lost from sample 2021JO5020C while splitting the 90–150 µm fraction for heavy mineral concentration for the ARTMin analysis. The remaining weight (57.1 g) was similar to the weight of the

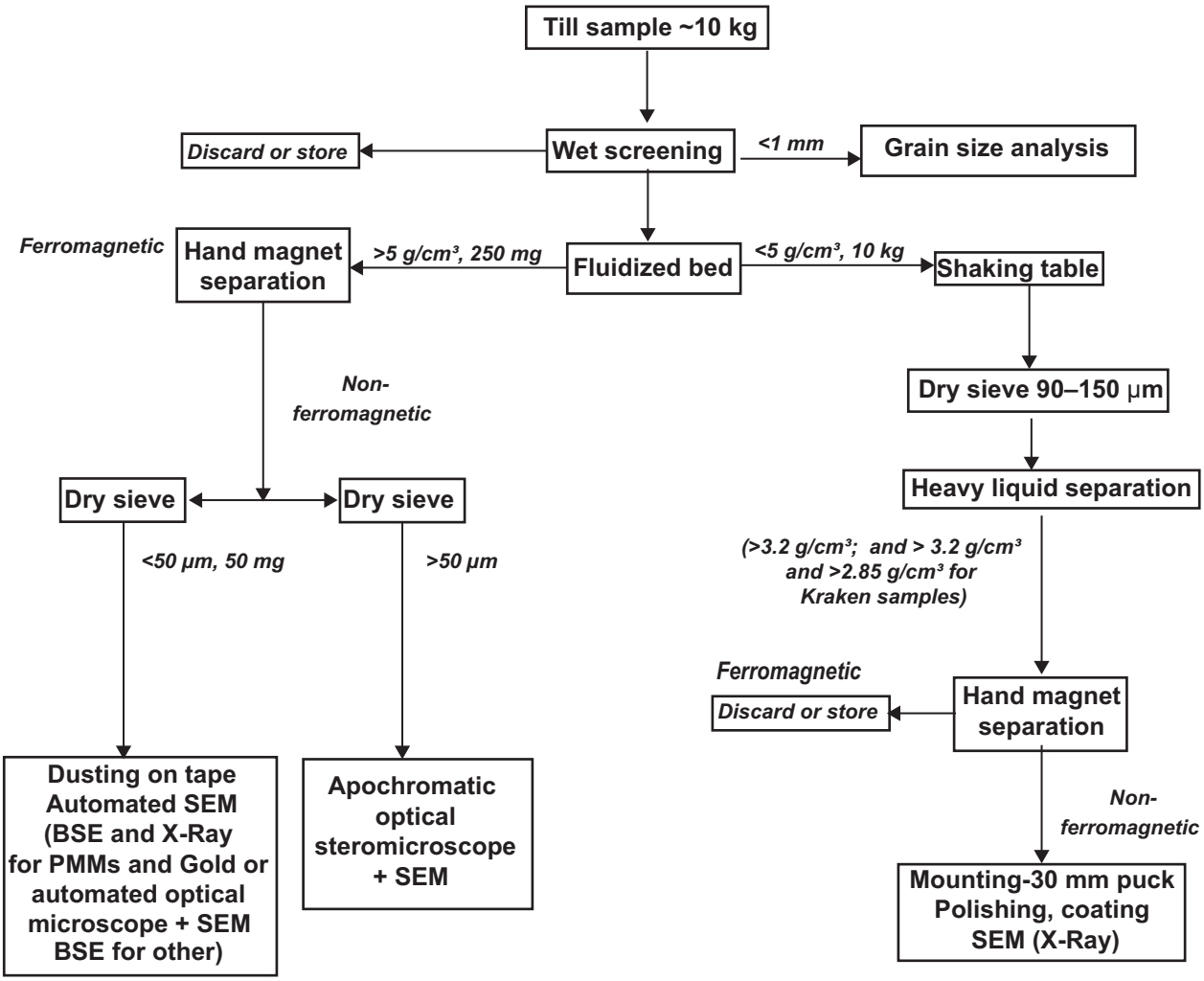

Figure 2. *Sample processing workflow for the samples from this study, modified after Girard* et al. *(2021a).*

90–150 µm fraction of the other till samples from this study and sufficient for heavy mineral separation and ARTMin analysis. Samples 2021JO5019A and 2021JO5020A lost slightly more weight (0.09 and 0.08 g) than the 0.05 tolerance value during magnetic separation, probably due to excessive clay agglomeration on individual grains that remained after acid washing.

The tailings from the fluidized bed used in the ARTGold analysis were rerun for sample 2021JO5019C with results indicating a 5% miss of the total amount of <50 µm grains at 5.5 g/cm^3 density, for a 95% recovery on the first run. The shaking table reject from the ARTMin analysis of sample 2021JO5020A was also rerun, and 10% visually re-scanned to determine how many minerals were missed from the first run. Rounded minerals show 100% recovery, but recoveries of minerals with square shapes or of lighter densities are variable.

ARTGold ANALYSIS

The instruments utilized for analysis include a high-definition SEM analyzer to improve resolution at low kilovolts (a Zeiss EVO MA15 HD with a LaB6 electron emitter equipped with an Oxford Instruments X-Max 150 mm2 energy dispersive spectrometer (EDS-SDD) and a Zeiss Sigma 300 VP field emission gun scanning electron microscope (FEG-STEM) coupled with the latest Oxford Instrument EDS-SDD Ultim-Max 170 mm^2 detector. A threshold is set with the back scattered electron (BSE) corresponding to a density of 5 g/cm^3. High resolution BSE images are recorded for each grain of gold and precious minerals and metals. Each grain is photographed and classified based on grain morphologies, ranging from pristine crystalline, pristine mutual, pristine intergranular, modified or remobilized grains using the ArtMORPH artificial intelligence (AI) image processing method verified by a trained geologist. Other dense minerals detected by BSE are scanned with the EDS and identified, but no image verification of the grain species is performed. Grain counts are estimated using pixel clusters, typically resulting in 30% overestimation (Natacha Fournier, pers. comm., 2025). As such, these results are considered semiquantitative.

ARTMin ANALYSIS

The samples are covered with a thin layer of carbon and scanned with the Zeiss Sigma 300 VP FEG-STEM equipped with an EDS-SDD for detection. The process is controlled by Aztec software including the detector controls, the acquisition of X-Ray maps, clustering algorithms and exporting of images. The ARTMin method only uses the X-ray spectra for mineral identification. X-Ray maps of pixels and output from the FE-SEM and EDS-SDD detectors are clustered using Aztec 4.2 software. Clusters of similar pixels are used to define mineral phases based on their chemical signatures. The individual spectra are subsequently manually examined to correct false peak labelling. Abundances of phases are computed as the number of pixels in a cluster versus the total number of non-blank pixels. Mineral names are determined by manual examination of the chemical formulas derived from the spectra, and by using MinIdent software (Smith and Leibovitz, 1986) for uncommon mineral phases.

RESULTS

GRAIN SIZE ANALYSIS

The sand, silt and clay proportions (Figure 3, Table 2) of all till samples analyzed fall within the expected range for lodgement/subglacial melt-out tills (Girard *et al.*, 2021b; Figure 3). The samples collected from southwest Newfoundland are 30% or more sandier than those from the northeast. The samples from the northeast contain high (14–37%) clay contents, whereas samples from the southwest contain high (53–58%) sand contents.

GOLD GRAIN MORPHOLOGIES

Pristine gold grains are mostly intergranular, suggesting they are derived from interstices of neighbouring minerals that are commonly found in intrusive or sheared metamorphic rocks (Girard *et al.*, 2021b). Grain morphology ranges from modified with rounded edges and silver dissolution pits, to pristine with irregular edges and angular surfaces; the latter suggesting nearby proximal sources with relatively small (<1 km) transport distances.

MINERALOGY

Tables 3–5 present the mineral abundances for gold grains (visual and automated), PMMs and other minerals (including granite-related minerals) detected in the <50 µm fraction, respectively. The abundance of gold and PMM grains reported in Figures 4–7 represent the normalized values (normalized to the weight of the <1000 µm sieved material) for comparison.

BURNT POND

The grain size distribution of the till samples indicates slightly lower clay contents in sample 2021JO5009A relative to sample 2021JO5009B (Figure 3). Gold grains are relatively abundant, with 66 grains recorded in the two till samples (123 grains when normalized to the weight of the <1000 µm concentrate). Modified gold grains account for 55–57% of gold grains (Figure 4A, Table 3). No distally derived (*i.e.*, reshaped) grains were detected in these sam-

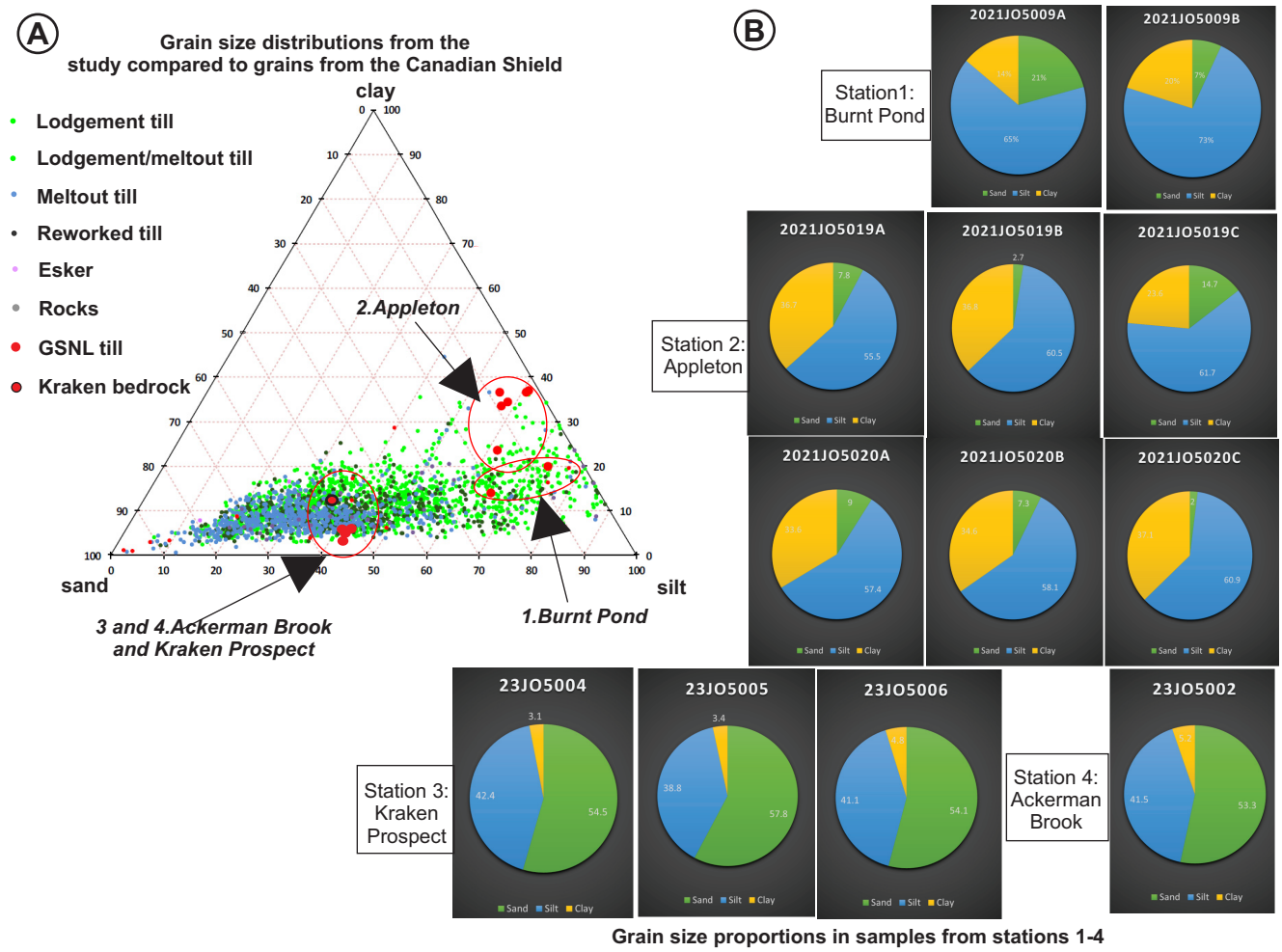

Figure 3. *A) Graph summarizing the sand, silt and clay percentages from this study compared to those collected in till overlying the Canadian Shield (Girard* et al.*, 2021b); B) Individual pie charts from each station showing the grain size proportions from samples (green–sand, blue–silt, yellow–clay).*

Table 2. Sand, silt and clay abundances in samples from stations and sections (where relevant) were sampled

Station	Area	Sample	Trench number or name	Sample depth (cm)	Till	Sand %	Silt %	Clay %
1	Burnt Pond	2021JO5009A	-	60	A	20.8	65.2	14
1	Burnt Pond	2021JO5009B	-	20	B	6.9	73	20.1
2	Appleton	2021JO5019A	1	300	A	7.8	55.5	36.7
2	Appleton	2021JO5019B	1	200	B	2.7	60.5	36.8
2	Appleton	2021JO5019C	1	70	C	14.7	61.7	23.6
2	Appleton	2021JO5020A	2	255	A	9	57.4	33.6
2	Appleton	2021JO5020B	2	160	B	7.3	58.1	34.6
2	Appleton	2021JO5020C	2	80	C	2	60.9	37.1
3	Kraken Prospect	23JO5004	East Dyke	50	B	53.3	41.5	5.2
3	Kraken Prospect	23JO5005	Hockey Stick Dyke	140	A	54.5	42.4	3.1
3	Kraken Prospect	23JO5006	Hockey Stick Dyke	65	B	57.8	38.8	3.4
4	Ackerman Brook	23JO5002	-	80	A	54.1	41.1	4.8

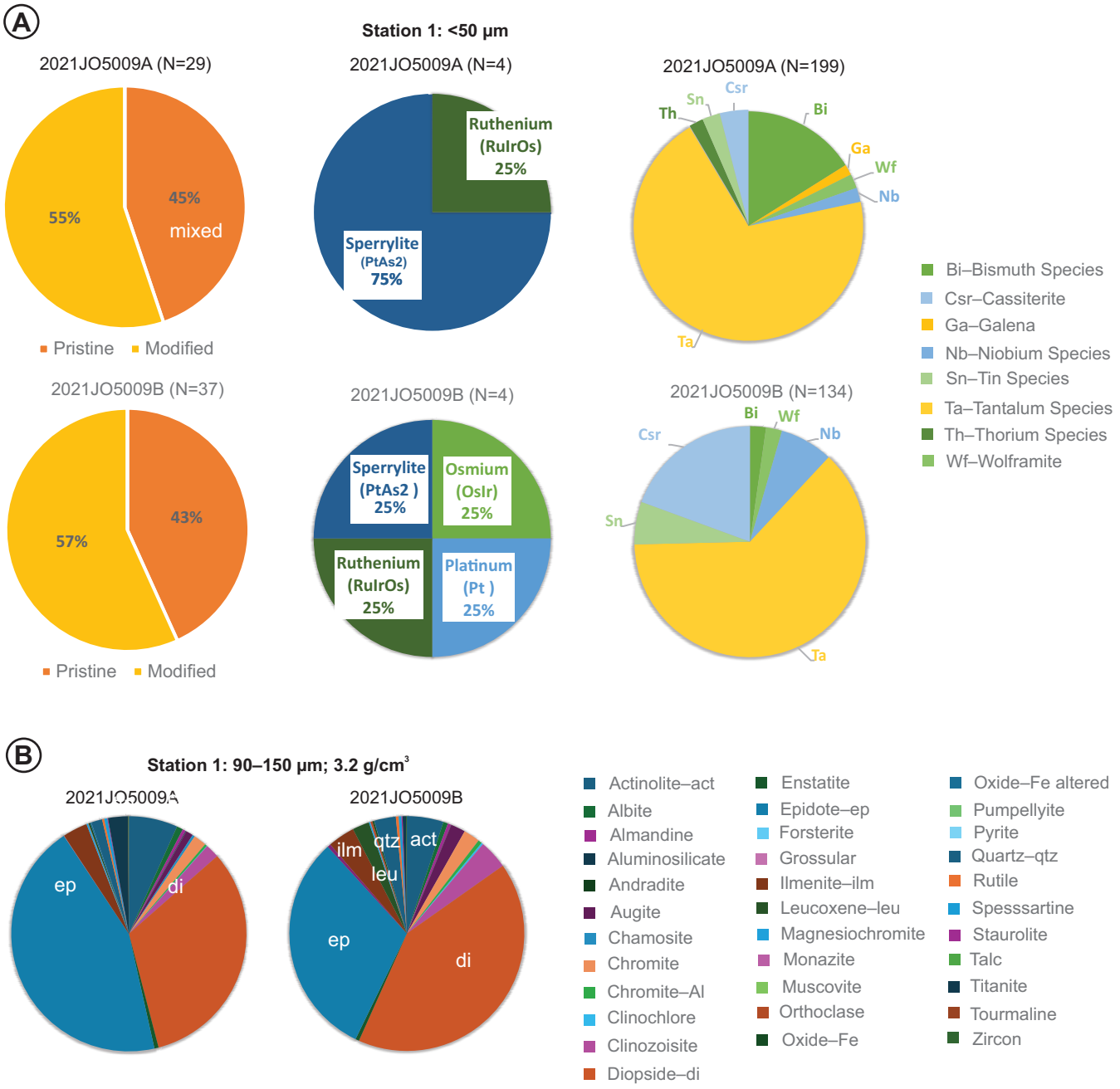

Figure 4. *A) Gold grain proportions (orange–pristine, yellow–modified), precious metal and mineral species, and granite-related minerals and mineral species in samples from Station 1; B) Proportion of minerals in the 90–150 µm fraction of samples from Station 1.*

ples. Pristine grains range in size from 15–40 µm, with the mobilized grains being slightly larger (20–50 µm). Gold chemistry, measured by EDS-SDD, indicates silver is a common alloy is detected in 56% of the grains; with six grains that are classified as electrum. The grains from sample 2021JO5009B have relatively less silver compared to those from sample 2021JO5009A and traces of copper and mercury are also detected.

Precious minerals and metal grains smaller than 30 µm were detected in both the upper and lower tills, with ruthenium and sperrylite in the lower till and osmium, platinum, ruthenium and sperrylite in the upper till (Figure 4A, Table 4). Bismuth and tantalum dominant mineral species (detected in both tills) are more abundant in sample 2021JO5009A (Figure 4A, Table 5), with higher tin and niobium dominant minerals and cassiterite grains in sample 2021JO5009B. Wolframite grain counts were similar for both units.

Table 3. Raw and normalized counts for gold grain morphology and abundances

Sample	Visual Evaluation 50–1000 µm	Automated Detection 0–50 µm	Total	Pristine	Modified	Reshaped	Undefined	Weight fine fraction <1 mm (kg)	Ratio grain/ kg (initial weight (W.S.)	Ratio grain/ 10 kg fraction <1 mm	Equivalent gold mass concentration
2021JO5009A	0	29	29	13	16	0	0	5.411	2.89	53.5	1.21
2021JO5009B	4	33	37	16	21	0	0	5.333	3.76	69.3	3.72
2021JO5019A	1	56	57	29	28	0	0	6.636	4.31	85.8	6.04
2021JO5019B	5	54	59	18	40	1	0	8.955	3.55	65.8	5.13
2021JO5019C	6	128	134	96	38	0	0	7.507	9.27	178.5	9.07
2021JO5020A	3	94	97	68	29	0	0	5.417	8.50	179.0	4.58
2021JO5020B	2	40	42	26	16	0	0	4.020	4.59	104.4	15.37
2021JO5020C	2	46	48	23	25	0	0	5.221	5.08	91.9	2.40
23JO5002	0	7	7	0	6	1	0	5.127	0.85	13.6	0.17
23JO5004	1	3	4	1	3	0	0	2.601	0.67	15.3	4.52
23JO5005	0	1	1	0	1	0	0	1.953	0.22	5.1	0.08
23JO5006	0	0	0	0	0	0	0	2.889	0.00	0.0	0.00
Bedrock KRAKEN 2023	0	0	0	0	0	0	0	13.067	0.00	0.0	0.00

Table 4. Raw and normalized grain counts for precious metals and minerals in the <50 µm fraction

Sample	Osmium (OS,Ir)	Platinum (Pt)	Rutheniridosmine (Os,Ir,Ru)	Ruthenium (Ru,Ir,Os)	Sperrylite (PtAs2)	Stibiopalladinite (Pd5+xSb2)	Total	Initial weight wet sieving (kg)	Ratio grain/ weight (W.S.)	Ratio grain/ 10 kg fraction 1 mm
2021JO5009A				1	3		4	10.019	0.4	7.3
2021JO5009B	1	1		1	1		4	9.833	0.4	7.5
2021JO5019A				3		1	4	13.231	0.3	6.0
2021JO5019B				1	1		2	16.633	0.1	2.2
2021JO5019C							0	14.456	0.0	0.0
2021JO5020A				2	2		4	11.411	0.4	7.3
2021JO5020B					1		1	9.145	0.1	2.4
2021JO5020C			1	1	1		3	9.447	0.3	5.7
23JO5002							0	8.246	0.0	0.0
23JO5004							0	5.952	0.0	0.0
23JO5005							0	4.498	0.0	0.0
23JO5006							0	4.278	0.0	0.0
Bedrock KRAKEN 2023							0	14.947	0.0	0.0

Table 5. Raw grain counts for other minerals detected in the <50 µm fraction of till samples

Sample	Bi-dominant	Hg-dominant	Galena	Pb-Oxide ?	Pb-Dominant	Scheelite	Wolframite	Nb-Dominant	Ta-Dominant	Th-Dominant	U-Dominant	Sb-Dominant	Sn-Dominant	Cassiterite	Cerianite	W-Dominant
2021JO5009A	32	0	3	0		0	4	4	139	4	0	0	5	8	0	
2021JO5009B	3	0	0	0		0	3	10	84	0	0	0	8	26	0	
2021JO5019A	6	0	0	0		0	4	6	63	3	0	0	14	17	0	
2021JO5019B	12	0	0	0		0	5	2	33	0	0	0	5	9	0	
2021JO5019C	3	0	0	0		0	5	4	24	7	0	0	10	8	0	
2021JO5020A	1	0	2	0		1	4	4	24	1	0	0	92	48	0	
2021JO5020B	11	1	0	0		0	12	0	46	4	1	0	48	20	0	
2021JO5020C	11	0	0	0		0	8	3	45	7	0	0	3	1	0	
23JO5002	39	0	0	0		37	52	0	30	50	1472	0	3	0	5	
23JO5004	56	0	0	0		28	182	5	355	13	7	0	7	5	0	
23JO5005	138	0	0	0		9	81	27	646	6	2	1	18	0	0	
23JO5006	50	0	0	1		1	111	37	549	5	1	0	6	5	0	
Bedrock KRAKEN 2023	15605				31			18	15150	1	298					2

The relative mineral abundances in the 90–150 µm fraction of >3.2 g/cm^3 mineral separates in the upper and lower tills are similar, with the most abundant minerals consisting of diopside, epidote, actinolite, clinozoisite and ilmenite (Figure 4B). The upper till has higher augite and leucoxene contents (>1% of total minerals identified), while the lower till is richer in titanite (2.7%). Numerous other minerals have been identified, including Al- and Mg-rich chromite and garnet (almandine > spessartine). The relative abundances of chromite, aluminum-rich chromite, and magnesium-rich chromite grains are 80:15:5 respectively, for both upper and lower till samples.

APPLETON

Sand, silt and clay percentages from samples 2021JO5019A and B and samples 2021JO5020B and C contain approximately the same ratios. The lower till layers contain 7–8% sand and the upper till layers contain 2–3% sand (Figure 3).

The bulk of gold grains are detected in the <50 µm fraction, (437 grains in 6 samples/526 grains normalized to the weight of the <1 mm concentrate; Figure 5A, Table 3). Despite the observation that the gold grains tend to be larger in bedrock (Eccles *et al.*, 2024), very few large grains (19) were recovered. Gold grain abundances and relative proportions of the pristine and modified grains are the same for samples 2021JO5019A and 2021JO5020C; and between 2021JO5019C and 2021JO5020B. Samples 2021JO5019C and 2021JO5020A contain the highest normalized gold grain counts. As with the gold grains at Burnt Pond, the pristine grains range from 15–40 µm, with the mobilized grains being similar to slightly larger (20–50 µm). The three largest grains (>150 µm) were identified from samples 2021JO5019A and C, and 2021JO5019B, while one remobilized grain (indicative of dispersal) was identified from sample 2021JO5019B (Table 3). Gold-grain chemistry, measured by EDS-SDD, indicates that silver is a significant alloy in many grains, detected in more than 70% of grains. Twenty grains are classified as electrum. As with the samples from Burnt Pond, trace amounts of copper and mercury are also detected.

In addition to gold grains, fourteen PMM grains (24 grains normalized) including ruthenium, rutheniridosmine, sperrylite and stibiopalladanite were identified in the <50 µm fraction of five of the six Appleton tills (Figure 5A, Table 4). Of these, the lowest till units contained the highest PMM counts with three grains of ruthenium and one stibiopalladanite (Pd_{5+x} Sb_{2-x}) in sample 2021JO5019A and two grains of ruthenium and two grains of sperrylite in sample 2020JO5020A. The sample 20212JO5020C contained one each of rutheniridosmine, ruthenium and sperrylite.

Granite-related minerals were more abundant in the lower till units, with 113 grains detected from sample 2021JO5019A and 177 grains in sample 2021JO5020A (Figure 5A (normalized values), Table 5). Tantalum and tin-dominant mineral species, including cassiterite, as well as wolframite were detected in the samples. High counts of tantalum and tin minerals were detected in sample 2021JO5019A, whereas high counts of tantalum and wolframite were detected in sample 2021JO5020B, and the highest counts of tin minerals were detected in sample 2021JO5020A.

The mineralogy of the 90–150 µm fraction of the 3.2 g/cm^3 density separates is variable, but the dominant minerals identified in all samples are oxidized iron sulphides, oxides, quartz, actinolite, ilmenite, leucoxene, augite, albite, almandine garnet, chromite and staurolite (Figure 5B). Oxidized pyrite is most abundant in the lowermost tills at both sample sites, with altered iron oxides in the upper till unit. Several other minerals are observed in trace amounts (<1% of the total minerals identified), including florencite (an altered apatite; $CeAl_3(PO_4)_2(OH)_6$) detected in four of the six till units, celadonite (a potassium–magnesium mica) detected in sample 2021JO5019A, and kaersutite ($NaCa_2(Mg_3Ti^{4+}Al)$ (Si_6Al_2) $O_{22}O_2$) detected in sample 2021JO5020B. Manganese-rich columbite occurs in sample 2021JO5020A. Monazite and rutile are 2–3 magnitudes more abundant in sample 2021JO5019C than all the other till samples, and allanite is also present in trace amounts.

KRAKEN PROSPECT

The clay, silt and sand percentages of the samples collected at the Kraken Prospect (Figure 3) are all similar; the till from the East Dyke upper sample (23JO5004) is almost identical to the upper till from the Hockey Stick Dyke (sample 23JO5006). The sand content of these samples is more than twice that of the samples from northeast Newfoundland.

Only five gold grains were identified in the three till samples (Figure 6A, Table 3); four of them are modified. No gold was identified in the spodumene-rich bedrock sample that was analyzed for comparison to the till samples. All of the gold contains minor (<4%) amounts of electrum. The <50 µm fraction of the three till samples are dominated by minerals typically associated with granite-related mineralization, namely scheelite, wolframite, and various unnamed thorium, uranium, bismuth, tin, niobium, and especially tantalum-dominated mineral species. Comparative mineral abundances indicate that scheelite, wolframite and thorium and uranium-dominant mineral species are roughly twice as abundant in the <50 µm fraction of till overlying the East Dyke *versus* the till from above the Hockey Stick Dyke

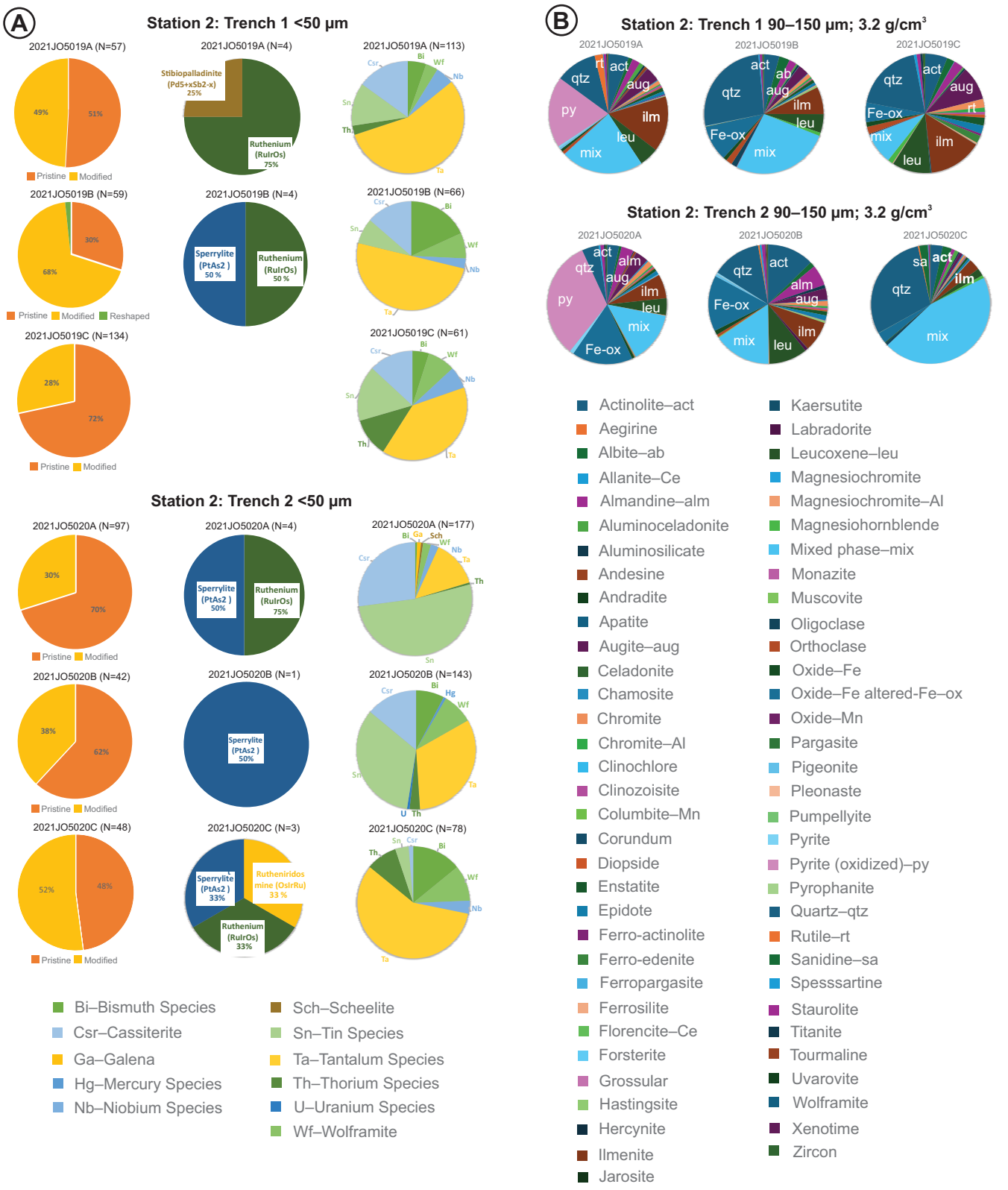

Figure 5. *A) Gold grain proportions (orange–pristine, yellow–modified), precious metal and mineral species, and granite related minerals and mineral species in samples from Station 2–trenches 1 and 2 and legends; B) Proportion of minerals in the 90–150 µm fraction of samples from Station 2–trenches 1 and 2; B) Proportion of minerals in the 90–150 µm fraction of samples from Station 2–trenches 1 and 2.*

(Figure 6A), and tantalum-rich mineral species are as also more abundant in the till from the East Dyke sample. The upper and lower tills at the Hockey Stick Dyke also show minor variations, with the lower till relatively enriched in scheelite and tantalum, bismuth and tin-dominated minerals, whereas the upper till is enriched in wolframite and niobium-dominant mineral grains. Over 30 000 grains of tantalum were estimated from the <50 µm fraction of the bedrock sample (Table 5).

Of the two heavy liquid separation densities (2.85–3.2 g/cm^3 and >3.2 g/cm^3) utilized for the till samples here, the

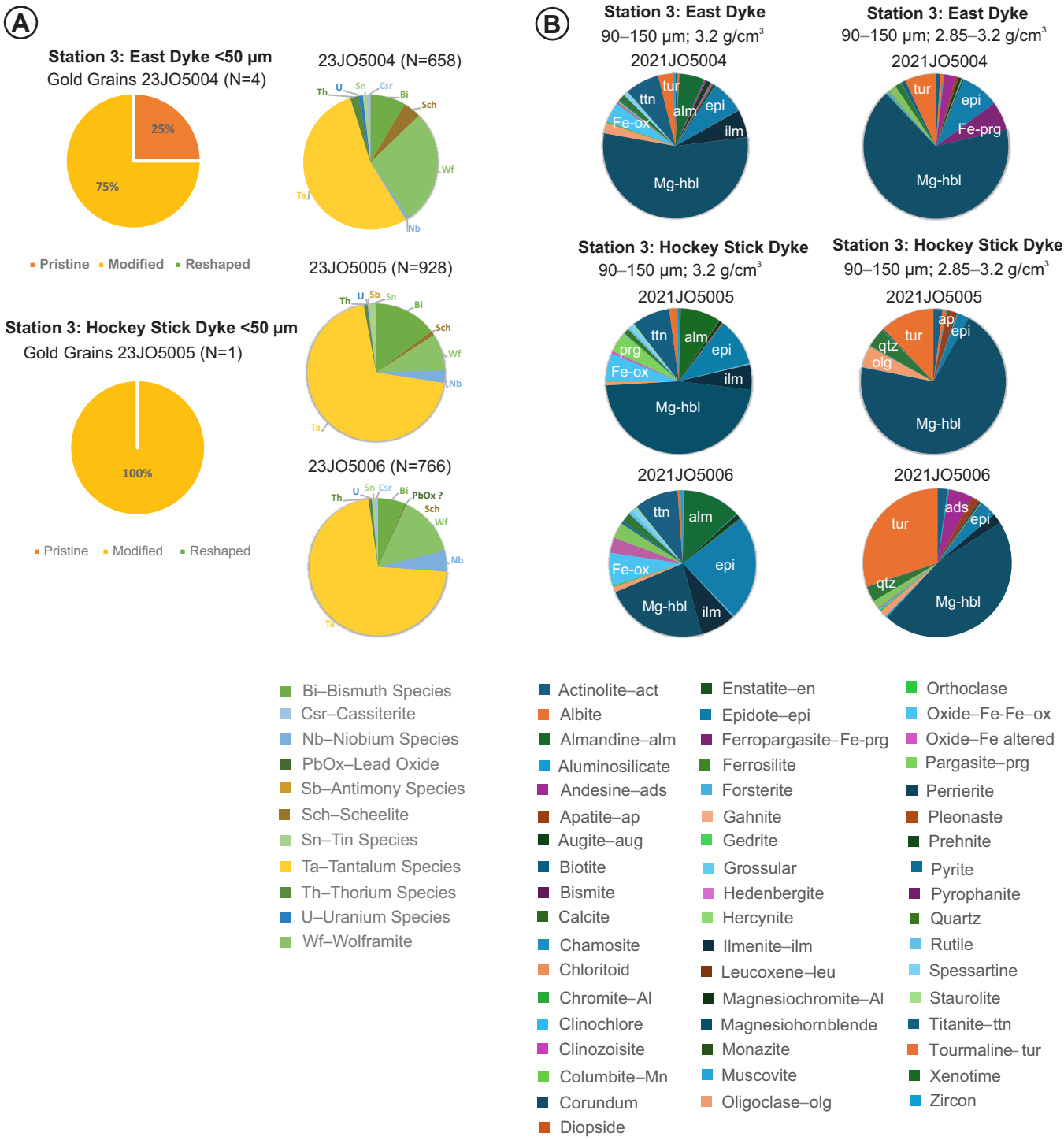

Figure 6. *A) Gold grain proportions (orange–pristine, yellow–modified), and granite related minerals and mineral species in samples from Station 3; B) Proportion of minerals in the 90–150 µm fraction of samples from Station 3.*

lighter fraction is relatively enriched in actinolite, apatite, biotite, clinozoisite, enstatite, magnesiohornblende, muscovite, oligoclase and tourmaline and the heavier fraction enriched in ilmenite, titanite, Fe-oxides and almandine and spessartine garnets (Figure 6B). The dominant minerals in each sample are similar, with amphiboles (magnesiohornblende and ferropargasite), epidote, tourmaline, almandine, feldspars, titanite and ilmenite most common. Significant trace minerals (<1% of the total mineral abundances) include staurolite, cordierite, columbite and rutile. Differences in the relative mineral abundances between the three samples, occur such as bismite (0.003%) and manganese columbite (0.004%) occurring only in tills overlying the East Dyke.

ACKERMAN BROOK

The distribution of sand, silt and clay in the till is similar to that of the Kraken Prospect and is almost exactly the same as the upper till unit from the Hockey Stick Dyke (Figure 3).

Seven gold grains, six of them modified, were identified from the <50 µm fraction of the 3.2 g/cm^3 density separate of till (Figure 7A, Table 3). Grain chemistry, measured by EDS-SDD, indicates that although silver is common, no electrum grains were identified. Abundant granite-related minerals were identified in the <50 µm till fraction, including scheelite, wolframite, thorium, cerianite (CeO_3) and over 1400 grains of an undifferentiated uranium species (Figure 7A).

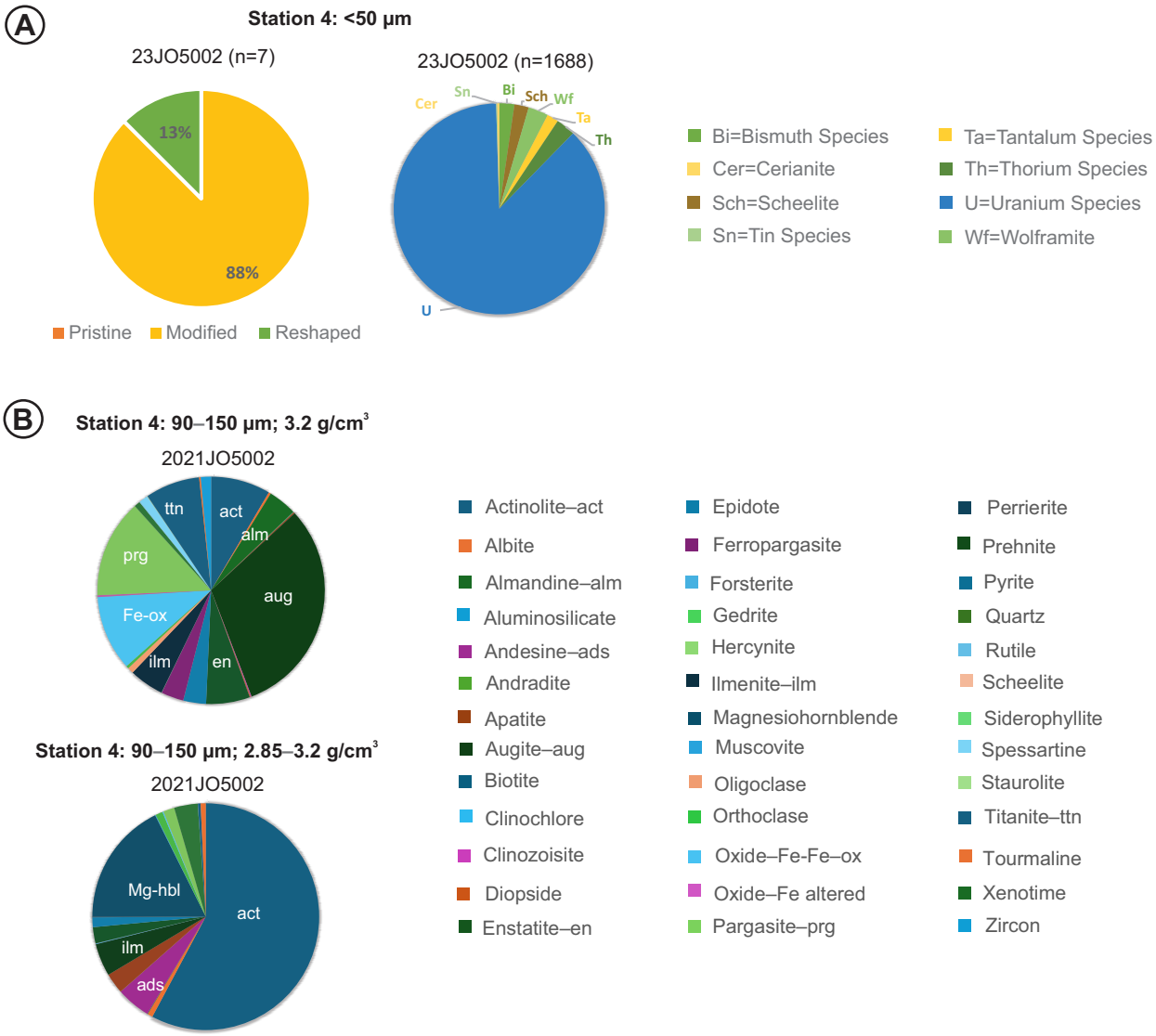

Figure 7. *A) Gold grain proportions (orange–pristine, yellow–modified), and granite related minerals and mineral species in samples from Station 4; B) Proportion of minerals in the 90–150 µm fraction of samples from Station 4.*

As at the Kraken Prospect, the 90–150 µm fraction of the till from Ackerman Brook was separated into a light (2.85 g/cm^3) and heavy (3.2 g/cm^3) fraction. In the light fraction, the dominant minerals were actinolite (57.8%) and magnesiohornblende (17.65%) with lesser andesine, augite, quartz, apatite and enstatite. The heavier fraction contains augite (31%), pargasite (13.97%), iron oxide (10.7%) and lesser actinolite, titanite, enstatite, ilmenite, almandine, epidote and ferropargasite (Figure 7B). In addition, trace to percent amounts of mafic minerals including diopside, epidote, hedenbergite and hercynite were identified. Spessartine, almandine and staurolite were also present, and andesine was recovered from the 2.85 g/cm^3 light mineral fraction. Trace perrierite, a Ca–Ti-sorosilicate (0.013%), pyrite (0.002%), and scheelite (0.002) were recovered using the 3.2 g/cm^3 density, and were also identified in the 90–150 µm fraction of the till sample.

DISCUSSION

GRAIN SIZE DISTRIBUTIONS

The grain size differences between till from northeast and southwest Newfoundland are most likely related to variations in the predominant compositions of bedrock sources. Fine- to medium-grained sedimentary rocks comprise a large portion of the bedrock in northeast Newfoundland, whereas coarse-grained granites predominate in southwest Newfoundland. The glacial environment of the northeast versus that of southwest may have also been a contributing factor, with at least 3 different recorded ice-flow orientations identified in an ice-marginal setting in the northeast, versus two ice-flow orientations identified in a (probable) inland setting in the southwest.

The upper tills (B and C) from Station 2, trench 2, were identified as lodgement tills based on fabric analysis, whereas tills B and C from Station 2, trench 1 were identified as subglacial melt-out tills (Organ, 2022). Based on their fissility and compactness, the other tills from this study could be either lodgement or subglacial melt-out tills. The grain size data support this assumption, with tills from Appleton containing anomalously high clay contents relative to tills of the southwest. The increased proportion of clay content is most likely attributed to the abundant, relatively easily eroded, sedimentary rocks in this region; but may also reflect the reworking of till samples by permafrost processes occurring in northeast Newfoundland between 11 000–10 000 years ago (Liverman *et al.*, 2000).

GOLD GRAIN MORPHOLOGIES

Studies of individual gold grain morphologies relating to glacial dispersal are ongoing. Preliminary results (based on the abundance of pristine grains with preservation of original grain faces and edges and lack of reshaping) indicate that the grains from stations 1 and 2 in northeast Newfoundland are close to their source. Conversely, samples from southwest Newfoundland, in stations 3 and 4 (Table 1), indicate some transport, with very few pristine grains identified relative to mobilized and reshaped grains.

While gold grain morphology is generally interpreted to reflect transport distances, other factors such as the host-rock composition and how the grain is glacially eroded and liberated are also important to consider (Girard *et al.*, 2021b). Three significant glacial erosion processes including permafrost, ice erosion and glaciomarine incursion (Campbell *et al.*, 2022; Organ, 2022) could contribute to the liberation of gold grains from bedrock sources in Appleton. However, the proximity of the grains in till samples to the Keats and Iceberg occurrences suggest they are locally derived.

BURNT POND

The distribution of sand, silt and clay, gold and PMM concentrations, and the ratio of pristine to modified gold grains are equal in the lower and upper till samples, suggesting the tills comprise a single unit (Figures 3 and 4A). The abundance of pristine gold grains would indicate local sourcing, whereas the modified grains indicate some transport, usually less than a kilometre (DiLabio, 1990). However, other factors, such as their original morphology and mode of occurrence in bedrock would need to be investigated before estimating transport distances (Girard *et al.*, 2021b). Although no known gold showings are located directly up-ice of the station location (*i.e.*, within <2 km), a few showings do occur in similar lithological settings in the Gander River Complex to the north of Burnt Pond, including the Jonathan's Pond Prospect (MODS 002E/02/Au001) and the Route 330 Gold Prospect (MODS 002E/02/Au037), and would suggest potential for future discoveries up-ice of the station site.

The PMM grains (Figure 4A) indicate the presence of an unknown local, or up-ice source. Forty percent of the PMMs in the tills (normalized grain counts) have chemical signatures that are associated with refractory PMM grains in ophiolites, while 60% are As- and Pt-rich PMMs commonly associated with serpentinization and hydrothermal alteration of chromatite (Zaccarini *et al.*, 2022). Whereas no known proximal sources exist for the PMMs, there are PMM indications in the Gander River Complex near Weirs Pond to the north of the station (MODS 002E/01/Pt/001–4; Bouzane, 2002). The significance of these grains is not known, but they could be used along with bedrock mineral assemblages, to characterize and detect detritus from ophiolite slivers that outcrop in this region.

The chromite grains and the predominance of minerals typically associated with mafic to ultramafic host rocks (*e.g.*, diopside, epidote, actinolite, ilmenite) in the 90–150 µm fraction (Figure 4B) is also consistent with these tills being partially sourced from the Gander River Complex. The upper till is also relatively enriched in minerals associated with low-grade metamorphism and hydrothermal alteration of mafic to ultramafic host rocks, such as leucoxene, clinochore, pumpellyite and talc. Their occurrence, as well as the high concentrations of chromite in the upper till suggest that they formed from northwest dispersal, supported by nearby disseminated chromite in hydrothermally altered talc–carbonate schist at Burnt Pond Point (MODS 002E/02/Cr003; Blackwood, 1980) ~1.5 km to the south-southeast, up-ice of the station. However, the abundance of granite-related mineral species in the <50 µm fraction would also suggest that north-northeast and north-northwest to northwesterly ice-flow events were vigorous enough to disperse material from granitic rocks, the most proximal of which occur south of Gander Lake, to the Burnt Pond station. Although the possible source(s) of these granite-related minerals is unknown, they highlight the potential of the Hunt's Pond, Gander Lake, Middle Ridge and Mount Peyton granites, and potentially unrecognized intrusions to host granite related critical mineral occurrences (*e.g.*, W, Sn, Bi, Ta).

APPLETON

Till samples from this station have the highest gold grain counts in this study, likely reflecting their proximity to known gold mineralization.

Given the abundance of pristine gold grains, and the minimal to zero content of remobilized grains, they are interpreted to be derived from proximal sources (Figure 5A). The most likely sources for gold grains in tills A and B at trench 1, and tills B and C at trench 2 are the Iceberg Zone to the west (MODS 002D/15/Au033), the 515 Zone to the south-southwest (MODS 002D/15/Au028) and the Keats North Zone to the southwest (MODS 002D/15/Au033). This interpretation is supported by clast fabrics and known ice-flow orientations (St. Croix and Taylor, 1991; Organ, 2022). The northeast to northwest flow identified in the lower units (*see* Appleton in Results), and north to northeast flow identified in the middle and upper units, at trench 2, contradicts the eastward and northeastward flow followed by northwestward flow recorded in the striation record. Thus, the interpretation of a simple subglacial emplacement of the upper tills at trench 2 by the relative ice-flow sequence does not fit with the data. Possible explanations for this discrepancy between clast fabric and striation measurements could include reworking of fabrics from mass wasting, the presence of a topographic obstruction causing a localized divergence in clast orientations, or the rafting of chunks of frozen debris with preserved northeast clast fabrics over till units with late-flow orientations.

Relatively few observable gold grains (<10% in the >50 µm fraction) were identified in till despite their abundant presence in bedrock of the Appleton linear (*e.g.*, Eccles *et al.*, 2024). If originally present in the till samples, these grains could have been too large for the initial <1 mm sieve, or, alternatively, they may not have been retained in the fluidized bed during the ARTGold shaking process (*see* Girard *et al.*, 2021a). It is unlikely that subglacial transport caused comminution, and the mixing of larger grains subglacially were responsible for the lack of large grains from probable up-ice (~100–150 m) source regions of the Keats and Iceberg prospects. Three of the larger (>150 µm) gold grains were identified in samples from here (Station 2); indicating larger grains could be more prevalent in this region relative to Burnt Pond. Optical gold grain studies, that have been historically used to define anomalous targets in this belt are recommended for the Appleton region given that they target larger gold grains, such as those observed in drillcore at Appleton (*e.g.*, Eccles *et al.*, 2024).

The economic and geological significance of the 14 (24 normalized) PMM grains in the <50 µm fraction from five of the six till samples (Figure 5B) is not yet understood. The grain chemistry indicates 55% refractory (osmium, ruthenium and iridium-type) PMMs and 45% secondary Sb and As-rich PMM grain species (Zaccarini *et al.*, 2022). The PMM grains, unlike gold, are more likely to survive large transport distances from sources (Makvandi *et al.*, 2021). As such, given the associated minerals and PMM mineral compositions, the PMMs could potentially be derived from units like the pyroxenites of the Gander River Complex. Alternatively, the PMMs could be sourced from lamprophyric dykes, similar to those from elsewhere in central Newfoundland (*e.g.*, Budgells Harbour (Reusch and Graves, 1988; Stuckless, 2008a, b). Similar kaersutite-bearing lamprophyritic dykes have been identified from Dildo Pond (Sandeman and Peace, 2024) and have been visually identified in the Appleton area (Cameron Peddle, pers. comm., August 2024); however, the exact locality of these dykes is difficult to determine as the observed outcrops are small (<2 m wide) and mostly disintegrated.

The abundance of granite-related minerals in the <50 µm fraction (Figure 5A) is consistent with sourcing of these minerals from granites located >10 km up-ice of the Appleton area. There are no known granite-related critical mineral occurrences in the immediate vicinity of the station; the granites south of Gander Lake are the most likely

source. The presence of foliated, equigranular muscovite–biotite–garnet-granite clasts in the upper tills of the Hunts Pond Granite (O'Neill and Colman-Sadd, 1993) would suggest a distal source upwards of 20 km to the southeast. Other potential sources ot the till indicator minerals include the peraluminous Middle Ridge Granite, as well as known tungsten mineralization at the Caribou River Tungsten showing (MODS 002D/10/W001), ~25 km south of the Appleton station.

Till C from trench 1 and Till B from trench 2 (Table 1) share the same relative abundances of the mafic to ultramafic associated minerals including actinolite, almandine, aluminum-rich chromite, clinozoisite, diopside, enstatite, epidote and staurolite (Figure 5B), indicating some compositional similarities between the two tills. The source for the minerals could be the Gander River Complex ~7.5 km to the southwest, where these minerals are abundant. Actinolite, enstatite and epidote are also common minerals in the Mount Peyton granodiorite to biotite–clinopyroxene–hornblende gabbro (Sandeman *et al.*, 2017), 14 km southwest of the station. Kaersuitite, along with clinopyroxene, chromite, magnetite, secondary chlorite and epidote are components of alkaline lamprophyre dykes, which occur just north of the study area, and have been identified in the Appleton area (Sandeman and Peace, 2024; Cameron Peddle, pers. comm., August 2024).

The sand, silt and clay percentages for tills A and B from trench 1 and tills B and C from trench 2 are similar (Figure 3). These till samples also share similar gold grain counts (Figure 5A), pristine to modified grain ratios, and abundances of aluminosilicates, ilmenite and monazite, suggesting they are correlative. However, granite-related mineral counts are higher in Till A of each trench, and generally decrease in upper till units.

The lower clay content of the upper till in trench 1 is consistent with its field interpretation of a supraglacial melt-out till (Organ, 2022). However, the combined silt and clay content of >80% suggests there was minimal water erosion (as would be expected in a supraglacial environment) of this unit. The observed disruption of pebble fabrics and the lack of compaction could have resulted from cryogenic mixing by permafrost. Oxidized pyrite grains that are most abundant in the lowest till units from both trenches, suggest that bedrock sources were exposed to the atmosphere, and possibly disaggregated by freeze-thaw processes, before glacial erosion and entrainment.

KRAKEN PROSPECT

In contrast to the till samples from the Burnt Pond and Appleton areas, the <50 μm fraction of till samples from the Kraken Prospect are characterized by very low total gold grain counts (<10 gold grains per sample), no PMMs and a much higher abundance of granite-related minerals (Figure 6A). The most likely source of the granite-related minerals in the till samples from the Kraken Prospect are either the underlying pegmatites (bedrock sample with >10 000 grains of Bi- and Ta-dominated minerals), or the abundant evolved peraluminous granites located to the north of the sample site (Rose Blanche and Peter Snout granites; Conliffe *et al.*, 2024).

The heavy (3.2 g/cm^3) and light (2.85 g/cm^3) 90–150 μm till fractions both reflect the underlying bedrock geology at the Kraken Prospect, with the abundant amphiboles, titanite and ilmenite sourced from amphibolites; pyrite from altered mafic to felsic tuffs surrounding the pegmatite dykes; and spessartine (and apatite?) sourced from the pegmatite dykes (Figure 6B). Local sourcing is consistent with the clast content of these tills, with tills containing abundant pebble to boulder sized clasts of the underlying rocks. Although spodumene was the predominant mineral recorded in the lighter fraction from the bedrock sample, none was detected by this method in the overlying tills. This is probably due to filtering of spodumene grains during the sample sieving process due to the large grain sizes (up to 12 cm; Conliffe *et al.*, 2024). Optical till-indicator mineral identification methods, such as those used at the North and South Brazil Lake LCT pegmatites in Nova Scotia (McClenaghan *et al.*, 2024a) are recommended for detecting spodumene in till derived from LCT pegmatites in the region. However, the methods used in this study are preferable for detecting other minerals associated with the deposits such as columbite–tantalum, as they are difficult to identify optically (McClenaghan *et al.*, 2024 b).

The identical sand, silt and clay percentages in the upper till units at both of the trenches suggests that the till horizon is continuous. However, there are differences in mineralogical assemblages between the units that may suggest some reworking of the upper till layers by later (southward?) ice flow. High sand contents have been recorded for hummocky landforms, as well as streamlined forms and featureless till veneer in the region (Sparkes, 1989, page 254). Results suggest that the higher sand content relative to samples from northeast Newfoundland, are related to the grain size of the underlying pegmatite and granitic bedrock rather than erosive processes.

ACKERMAN BROOK

The Ackerman Brook till, despite being collected from a different landform as the upper till unit from the Kraken Prospect (Sample 23JO5006), has the same sand, silt and clay percentages (Figure 3). These results fit with those of

previous studies (Sparkes, 1989) concluding that the grain size distribution was almost identical for hummocks, streamlined landforms and till veneer. Despite this region having been previously explored for its gold potential (Walker and Robinson, 1986), very few gold grains were identified relative to samples from the northeast (Figure 7A, Table 3), and the grains that were identified were modified, indicating transport. It is unlikely that they were transported 4 km northeastward from the Cross Gulch showings, or northwestward from the Couteau Brook showings but the general lack of ice-flow indicators hampers interpretation of their provenance ice-flow reconstruction and glacial-dispersal models.

The <50 μm till fraction is characterized by a very high abundance of U-dominated minerals, which account for 87% of the total grains identified (Figure 7A). A number of uranium showings are located in the Dolman Cove Formation and Piglet Brook Rhyolite to the north of the sample site, as well as the Troy's Pond and ST-129 showings (MODS 011O/16/U 001-002; Kahlert *et al.*, 2008), about 10 km west of the Ackerman Brook sample site. Although it is unlikely that these U-rich minerals were directly sourced from these showings due to the dominant southerly ice-flow direction, they highlight the potential for other occurrences in the same host rocks north of the sample site and east along strike from known showings. The presence of other granite-related minerals such as scheelite, wolframite, thorium and cerianite (CeO_2), may be related to evolved peraluminous granite bodies mapped north of the sample site, and highlight the granite-related critical mineral potential of this area.

The 90–150 μm fraction is dominated by amphiboles and pyroxenes (actinolite and magnesiohornblende in the light fraction, and augite and pargasite in the heavy fraction (Figure 7B)), which were likely sourced from the Ironbound Hill intrusion (O'Brien *et al.*, 1986), ~3 km north of the sample site. The diopside, enstatite, epidote, hedenbergite, ferroparagasite and hercynite could also have been dispersed from this potential source southward. Spessartine and scheelite could be dispersed from evolved intrusive units (peraluminous granites and associated pegmatites), while staurolite has been recorded in the metamorphosed Dolman Cove Formation to the north of the station (Chorlton, 1980b). As this sample was the only one collected randomly, the results are significant and should be investigated further. Surface sampling from this region is warranted given its critical mineral potential.

FUTURE WORK

This work highlights the potential of the ARTGold and ARTMin methods to effectively detect minerals from vein, ultramafic and pegmatite and granite-hosted showings, indications and prospects. Further work would characterize (probable) up-ice bedrock units to compare the results with grains detected in till. For instance, the Middle Ridge, Gander Lake, Hunt's Pond and Mount Peyton granitic units up-ice of the Appleton and Burnt Pond stations, should be characterized through SEM, to determine the ratios of tin, columbite–tantalite and tungsten minerals. The ratios should be compared to those in the lower and upper till units from this study. This could assist in narrowing down the sources of mineralization in till and help constrain ice-flow vectors for exploration work in this area. Similarly, till mineralogical samples collected distal to known indications, prospects and showings at the Kraken Prospect could also help constrain ice-flow vectors or detect mineralogical contributions from buried pegmatites.

SUMMARY

Both the ARTGold and ARTMin methods using scanning electron microscope and automated identification of indicator minerals, successfully detected minerals from the < 50 μm and 90–150 μm fractions of till samples overlying and proximal to gold and LCT pegmatite mineral indications, showings, and prospects in Appleton and Kraken.

In addition, the ARTGold method detected abundant PMMs and columbite–tantalite, wolframite, cassiterite and Bi, Ta, Nb, Sn and U-dominant mineral species in the <50 μm fraction. This method could be used to determine the distribution of elements relating to critical minerals, such as Pt, Pd, Bi, Ta, Nb, Sn, U, Ru, Mo, Sn and W in tills. These minerals were detected in tills >10 km from granites and ultramafic units in the Burnt Pond and Appleton region.

The detection and identification of bedrock minerals (*e.g.*, diopside, enstatite, spessartine, tourmaline) in the 90–150 μm fraction are sufficient in abundance to aid in identifying bedrock contributions. Furthermore, the detection of multiple species of minerals and their chemistry helps better discriminate possible bedrock sources for the tills, and their associated mineralization (*e.g.*, Makvandi *et al.*, 2021). While the methods utilized here are specific to finer grained mineral species, the relative abundance and composition of granite minerals in till can be compared to till abundances of wolframite, cassiterite, tungsten and other granite-hosted minerals to help differentiate and trace detritus to specific bedrock sources, as can the abundances of mafic bedrock-hosted minerals. Thus, the analytical methods used here could greatly assist exploration efforts by helping to elucidate variable inputs of different till detritus by utilizing the detailed mineralogical data in addition to traditional till geochemical data.

Further studies, using the scanning electron microscope detection of the fine fraction of tills could be used, together with bedrock studies, to fully characterize the mineralogy of till overlying mineralogically prospective geological terranes.

ACKNOWLEDGMENTS

Rashmi Hazarika is thanked for cartographic support, and John Hinchey for his discussions and comments that greatly clarified some of the concepts in this paper. Joanne Rooney is commended for her excellence in compositing this manuscript. The authors appreciate Newfound Gold Corp and Benton Resources Corp for granting permission to sample on their properties, and to Barry Sparkes who provided bedrock samples for comparison. Natacha Fournier and the staff at IOS Geosciences are much appreciated for their expertise and explanations throughout the study.

AUTHOR CONTRIBUTIONS

Heather Campbell – conception, writing, analytical design, site observations for the 2023 samples; Jennifer Organ – sampling, site observations; James Conliffe – field observations, mineral deposit and bedrock history and emplacement.

REFERENCES

Blackwood, R.F.
1979: Gander River, Newfoundland. Government of Newfoundland and Labrador, Department of Mines and Energy, Mineral Development Division, Map 79-029, Geofile 002E/0304

1980: Gander River, Newfoundland. Map 80-031. Government of Newfoundland and Labrador, Department of Mines and Energy, Mineral Development Division, Open File 2E/02/0412.

Bouzane, J.
2002: First year assessment report on prospecting and geochemical exploration for licence 7929M on claims in the Muddy Gullies area, near Weirs Pond, northeastern Newfoundland. Newfoundland and Labrador Geological Survey, Assessment File 2E/01/1186, 34 pages.

Campbell, H.E.
2024: Till-indicator mineral dispersal and ice flow in the northern Hopedale Block: Implications for mineral exploration. *In* Current Research. Government of Newfoundland and Labrador, Department of Industry, Energy and Technology, Geological Survey, Report 24-1, pages 105-125.

Campbell, H.E., Sandeman, H. and Organ, J.
2022: Glaciotectonic deformation along a 70 km section of the Dog Bay Line: Beaver Brook Antimony Mine to Ten Mile Lake. *In* Current Research. Government of Newfoundland and Labrador, Department of Industry, Energy and Technology, Geological Survey, Report 22-1, pages 157-181.

Chen, D., Miyamoto, A. and Keneko, S.
2013: Robust surface reconstruction in SEM using two BSE detectors. IEICE Transactions on Information and Systems, Volume E96.D, Issue 10, pages 2224-2234

Chorlton, L.
1980a: Geology of the La Poile River area (11O/16), Newfoundland. Government of Newfoundland and Labrador, Department of Mines and Energy, Mineral Development Division, Report 80-3, 96 pages.

1980b: Peter Snout, west half. *In* Current Research. Government of Newfoundland and Labrador, Department of Mines and Energy, Mineral Development Division, Report 80-1, pages 62-73.

Conliffe, J. Archibald, D.B. and Sparkes, B.A.
2024. Lithium–cesium–tantalum (LCT) pegmatites in southwestern Newfoundland. *In* Current Research. Government of Newfoundland and Labrador, Department of Industry, Energy and Technology, Geological Survey, Report 24-1, pages 31-52.

Dickson, W.L.
1993: Geology of the Mount Peyton map area (NTS 2D/14), central Newfoundland. *In* Current Research. Government of Newfoundland and Labrador, Department of Mines and Energy, Geological Survey Branch, Report 93-1, pages 209-220.

Dilabio, R.N.W.
1990: Classification and interpretation of the shape and surface textures on the Canadian Shield. *In* Current Research, Part C. Geological Survey of Canada, Paper 90-1C, pages 323-329.

Eccles, D.R., Jorgensen, M.K. and Simmons, G.
2024: New Found Gold Corp's Queensway Gold Project in Newfoundland and Labrador, Canada: 2024 exploration update technical report.
https://www.sedarplus.ca/csa-party/records/document.html?id=9573ab241de5c65a3bac4a4c1260f3537cf2ebe58304dbcadc3f1acca744f9d0

Evans, D.J.A., Phillips, E.R., Hiemstra, J.F. and Auton, C.A.
2006: Subglacial till: Formation, sedimentary characteristics and classification. Earth Science Reviews, Volume 78, pages 115-176. https://doi.org/10.1016/j.earscirev.2006.04.001

Girard, R.., Tremblay, J., Néron, A., Longuépée, H.
2021a: Automated Gold Grain Counting. Part 1: Why Counts Matter! Minerals Volume 11, Article 337. https://doi.org/10.3390/min11040337

Girard, R., Tremblay, J., Néron, A., Longuépée, H. and Makvandi, S.
2021b: Automated gold grain counting, Part 2: What a gold grain size and shape can tell! Minerals, Volume 11, Article 379. https://doi.org/10.3390/min11040379

Gu, Y.
2003: Automated scanning electron microscope based mineral liberation analysis. An introduction to JKMRC/FEI Mineral Liberation Analyser. Journal of Minerals & Materials Characterization & Engineering, Volume 2, Number 1, pages 33-41. https://www.scirp.org/pdf/JMMCE20030100003_64231986.pdf

Honsberger,.I.W., and Sandeman, H.A.I.
2023: Geological overview of the Dog Bay Line-Appleton Fault zone gold corridor, northeast-central Newfoundland, Canada. Atlantic Geoscience Abstracts-Geological Association of Newfoundland and Labrador Section-2023 Technical Meeting. Volume 59, Number 75, pages 2564-2987. https://doi.org/10.4138/atlgeo.2023.003

Kahlert, B.H., Hitchcock, D. McGarry, T.G. and Scott, W.J.
2008: Second year supplementary and third year assessment report on geochemical, geophysical and trenching exploration for licences 10851M and 12359M on claims in the Troys Pond area, southwestern Newfoundland. Commander Resources Limited, Quinlan, R and Quinlan, E. Newfoundland and Labrador Geological Survey, Assessment File 11O/16/0407, 2008, 103 pages.

Layton-Matthews, D. and McClenaghan, M.B.
2022: Current techniques and applications of mineral chemistry to mineral exploration; examples from glaciated terrain: A review. Minerals, Volume 12, Issue 59.

Liverman, D., Catto, N., Batterson, M., Mackenzie, C., Munro-Stasiuk, M., Scott, S. and Somerville, A.
2000: Evidence of Late Glacial Permafrost in Newfoundland, Quaternary International, Volumes 68–71, pages 163-174. https://doi.org/10.1016/S1040-6182(00)00041-0.

Lougheed, H.D., McClenaghan, M.B., Layton-Matthews, D., Leybourne, M.I. and Dobosz, A.N.
2021: Automated indicator mineral analysis of fine-grained till associated with the Sisson W-Mo Deposit, New Brunswick, Canada. Minerals, Volume 11, Issue 2, Article 103. https://doi.org/10.3390/min11020103

Makvandi, S., Pagé, P., Tremblay, J. and Girard, R.
2021: Exploration for platinum-group minerals in till: A new approach to the recovery, counting, mineral identification and chemical characterization. Minerals, Volume 11, Issue 3, Article 264. https://doi.org/10.3390/min11030264

McClenaghan, M.B., Parkhill, M.A., Pronk, A.G. and Sinclair, W.D.
2017: Indicator mineral and till geochemical signatures of the Mount Pleasant W-Mo-Bi and Sn-Zn-In deposits, New Brunswick, Canada. Journal of Geochemical Exploration, Volume 172, pages 151-166.

McClenaghan, M.B., Brushett, D.M., Beckett-Brown, C.E., Paulen, R.C., and Rice, J.M.
2024a: Indicator minerals for lithium exploration in glaciated terrain. Explore newsletter for the Association of Applied Geochemists, Number 203, https://doi.org/10.70499/BFKH4666

McClenaghan, M.B., Brushett, D.M., Beckett-Brown, C.E., Paulen, R.C., Rice, J.M. and White, C.
2024b. Indicator mineral data for till and bedrock samples from the Brazil Lake pegmatite area, southwest Nova Scotia (NTS 21A/04, 20-O/16 and 20P/13). Geological Survey of Canada, Open File 9189.

O'Brien, S.J., Dickson, W.L. and Blackwood, R.F.
1986: Geology of the central portion of the Hermitage Flexure area, Newfoundland. *In* Current Research. Government of Newfoundland and Labrador, Department of Mines and Energy, Mineral Development Division, Report 86-1, pages 189-208.

O'Brien, B.H. and O'Brien, S.J.
1989: Geology of the western Hermitage Flexure: Bay D'Est Fault and south (parts of 11O/9, 11O/16, 11P/12 and 11P/13), southwest Newfoundland. Map 89-133. Government of Newfoundland and Labrador, Department of Mines and Energy, Geological Survey, Open File NFLD/1905.

O'Neill, P.P. and Blackwood, R.F.
1989: A proposal for revised stratigraphic nomenclature of the Gander and Davidsville Groups and the Gander River Ultrabasic Belt of northeastern Newfoundland. *In* Current Research. Government of Newfoundland and Labrador, Department of Mines, Geological Survey, Report 89-1, pages 127-130.

O'Neill, P.P. and Colman-Sadd, S. P.
1993: Geology of the eastern part of the Gander (NTS 2D/15) and western part of the Gambo (NTS 2D/06) map areas, Newfoundland. Government of Newfoundland and Labrador, Department of Mines and Energy, Geological Survey Branch, Report 93-02, 53 pages.

Organ, J.
2022: Northwest Gander surficial mapping project: preliminary investigations. *In* Current Research. Government of Newfoundland and Labrador, Department of Industry, Energy and Technology, Geological Survey, Report 22-1, pages 211-235.

Plouffe, A, Lee, R.G., Byrne, K., Kjarsgaard, Petts, D.C., Wilton, D.H.C., Ferbey, T. and Oelze, M.
2024: Tracing detrital epidote derived from alteration halos to porphyry Cu deposits in glaciated terrains: The search for covered mineralization. Economic Geology Volume 119 Number 2, pages 305-329. https://doi.org/10.5382/econgeo.5049

Reusch, D. and Graves, G.
1988: First year assessment report on geological and geochemical exploration for licence 3023 on claim block 5100 and licence 3030 on claim block 5012 in the Budgell Harbour area, northern Newfoundland. Newfoundland and Labrador Geological Survey, Assessment File 2E/06/0592, 25 pages.

Sandeman, H.A.I. and Peace, A.L.
2024: Petrochemistry, mineralogy, and Nd isotopic analyses of Tithonian alkaline lamprophyric intrusions, north-central Newfoundland, Canada. Canadian Journal of Earth Sciences, Volume 62, Number 1. https://doi.org/10.1139/cjes-2024-0087

Sandeman, H.A.I., Dunning, G.R., McCullough, C.K. and Peddle, C.
2017: U–Pb chronology, petrogenetic relationships and intrusion-related precious-metal mineralization in the northern Mount Peyton Intrusive Suite: Implications for the origin of the Mount Peyton Trend, central Newfoundland (NTS 2D/04). *In* Current Research. Government of Newfoundland and Labrador, Department of Natural Resources, Geological Survey, Report 17-1, pages 189-217.

Sandeman, H. and Honsberger, I.
2023: Gold mineralization at the Valentine Lake, Moosehead, Queensway and Kingsway projects. Geological Association of Canada, Newfoundland and Labrador Fall Field trip 2023. Unpublished, https://www.gac-nl.ca/guidebooks

Shaw, J., Piper, D.J.W., Fader, G.B., King, E.L., Todd, B.J., Bell, T., Batterson, M.J. and Liverman, D.G.E.
2006: A conceptual model of the deglaciation of Atlantic Canada. Quaternary Science Reviews, Volume 25, pages 2059-2081.

Smith, D.G.W. and Leibowitz, D.
1986: MinIdent: A database for minerals and a computer program for their identification. Canadian Mineralogist, Volume 24, pages 695-708.

Sparkes, B.G.
1989. Quaternary geology of southwestern Newfoundland. *In* Current Research. Government of Newfoundland and Labrador, Department of Mines, Geological Survey, Report 89-1, pages 249-257.

Sparkes, B.G. and McCuaig. S
2005: Surficial geology of the Peter Snout map sheet (NTS 11P/13). Map 2005-43. Government of Newfoundland and Labrador, Department of Natural Resources, Geological Survey, Open File 11P/13/0208.

St. Croix, L. and Taylor, D.M.
1991: Regional striation survey and deglacial history of the Notre Dame Bay area, Newfoundland. *In* Current Research. Government of Newfoundland and Labrador, Department of Mines and Energy, Geological Survey Branch, Report 91-1, pages 61-68.

Stuckless, E.
2008a: First, third- and sixth-year assessment report on geochemical, geophysical and diamond drilling exploration for licences 8279 M, 10592 M, 10667 M, 10750 M, 10839 M, 12701 M, 12923 M, 13345 M, 13353 M and 13355M-13356 M on claims in the Budgells Harbour area, north-central Newfoundland, 2 reports. Newfoundland and Labrador Geological Survey, Assessment File 2E/1669, 404 pages.

2008b: Second and third year and sixth year supplementary assessment report on geochemical and diamond drilling exploration for licences. 8279 M, 10592 M, 10667 M, 10750 M, 10839 M, 12701 M, 12923 M,

13345 M, 13353 M and 13355M-13356 M on claims in the Budgells Harbour area, north-central Newfoundland. Newfoundland and Labrador Geological Survey, Assessment File 2E/1586, 2008, 163 pages.

Walker, S.D. and Robertson, K.
1986: Second year assessment report on prospecting, geological, geochemical and geophysical exploration for licence 2491 on claim blocks 2419 and 2425 and licence 2885 on claim blocks 3737-3742 in the Cross Gulch and East Bay Brook areas, southwestern Newfoundland. Noranda Exploration Company Limited and Granges Exploration Limited Newfoundland and Labrador Geological Survey, Assessment File NFLD/1535, 1986, 31 pages.

Zaccarini, F., Economou-Eliopoulos, M., Kiseleva, O., Garuti, G., Tsikouras, B., Pushkarev, E. and Idrus, A.
2022: Platinum group elements (PGE) geochemistry and mineralogy of low economic potential (Rh-Pt-Pd)-rich chromitites from ophiolite complexes. Minerals 2022, Volume 12, Article 1565.
https://doi.org/10.3390/min12121565